

# Acid–Base Properties of the (1-4,18-36) Fragments of Neuropeptide K and their Mono- and Polynuclear Copper(II) Complexes Products of Metal-Catalyzed Oxidation

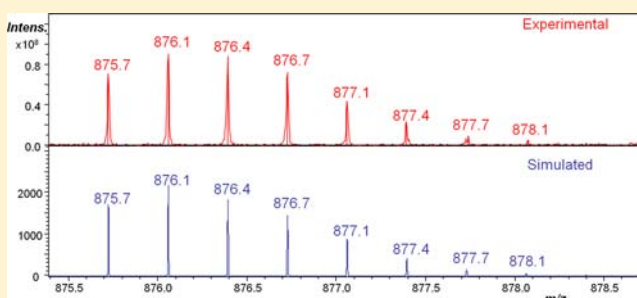
Marta Błaszczak,<sup>†</sup> Elżbieta Jankowska,<sup>‡</sup> and Teresa Kowalik-Jankowska<sup>\*,†</sup>

<sup>†</sup>Faculty of Chemistry, University of Wrocław, 14 Joliot-Curie, 50-383 Wrocław, Poland

<sup>‡</sup>Faculty of Chemistry, University of Gdansk, 18 Sobieskiego, 80-952 Gdansk, Poland

## Supporting Information

**ABSTRACT:** Mononuclear and polynuclear complexes of the (1-4,18-36)NPK, Asp<sup>1</sup>-Ala-Asp-Ser<sup>4</sup>-Gly<sup>18</sup>-His<sup>19</sup>-Gly-Gln-Ile-Ser-His<sup>24</sup>-Lys-Arg-His<sup>27</sup>-Lys-Thr-Asp-Ser-Phe-Val-Gly-Leu-Met<sup>36</sup>-NH<sub>2</sub>, and mononuclear complexes of its acetyl derivative Ac-Asp<sup>1</sup>-Ala-Asp-Ser<sup>4</sup>-Gly<sup>18</sup>-His<sup>19</sup>-Gly-Gln-Ile-Ser-His<sup>24</sup>-Lys-Arg-His<sup>27</sup>-Lys-Thr-Asp-Ser-Phe-Val-Gly-Leu-Met<sup>36</sup>-NH<sub>2</sub> have been studied by potentiometric, UV–vis, CD, EPR spectroscopic, and mass spectrometry (MS) methods. As it was observed for other tachykinins (neurokinin A, neuropeptide gamma and its fragments) containing the same C-terminal sequence His-Lys-Thr-Asp-Ser-Phe-Val-Gly-Leu-Met-NH<sub>2</sub>, also for the fragments of neuropeptide K the additional deprotonation most likely on the serine OH group was observed. It is likely that tachykinin peptides contain catalytic Ser/His/Asp triad or dyads Ser/Lys and the serine protease activity. The high water solubility of the resulting metal complexes allowed us to obtain complete complex speciation at different metal-to-ligand ratios ranging from 1:1 to 4:1 for (1-4,18-36)NPK, while only the 1:1 molar ratio was studied for Cu(II)–Ac-(1-4,18-36)NPK because of precipitation. For the metal-to-ligand 1:1 molar ratio the (1-4,18-36)NPK forms in a wide 6.5–10.5 pH range the CuHL complex with a 3N {NH<sub>2</sub>,2N<sup>−</sup>,β-COO<sup>−</sup>-Asp<sup>3</sup>} binding site. For a metal-to-ligand 1:1 molar ratio at higher pH than 9.5 the dimeric species dominate. For the Ac-(1-4,18-36)NPK peptide the imidazole nitrogen atoms are the primary metal-binding sites forming macrochelates in the pH 4 – 7.5.



## INTRODUCTION

Neuropeptide K (NPK), a 36 amino acid residue, tachykinin peptide, with neurokinin A (NKA) at its C terminus, has been isolated from porcine brain<sup>1</sup> and regarded as a specific post-translational product of PPT-A gene.<sup>2,3</sup> NPK is the major tachykinin in the cerebral cortex and hippocampus. The amino acid sequence of neuropeptide K is as follows:

### NPK DADS<sup>4</sup>SIEKQVALLKALYGH<sup>19</sup>GQISH<sup>24</sup>KRH<sup>27</sup>KTDSF- VGLM<sup>36</sup>-NH<sub>2</sub>

A comparison of the primary structure of this 36-amino acid-containing peptide from bovine,<sup>4</sup> human,<sup>5</sup> porcine,<sup>1</sup> and rat species reveals a striking sequence homology of 97–100%. Tachykinins exert their biological effects by binding them to specific receptors belonging to the protein-linked receptor family. Three subtypes of receptors have been described, named NK1 (substance P, SP-preferring), NK2 (neurokinin A, NKA-preferring), and NK3 (neurokinin B, NKB-preferring) subtypes. In the rat, the genes encoding for NK1, NK2, and NK3 are located in chromosomes 4, 20, and 2, respectively.<sup>7</sup> Neuropeptide K has been shown to have high selectivity for the NK2 receptor. Studies indicate that NPK represents thus far the

most potent and longest lasting vasodepressor and cardiomodulatory tachykinin, whose actions appear to be mediated by direct action on blood vessels and the autonomic nervous system, respectively.<sup>8</sup> NPK is involved in contracting the gall bladder, causing protein extravasation, hypotension, and bronchial smooth muscle spasms.<sup>2</sup> A important role of NPK in the nerve terminal region is to provide a pool or reservoir of the peptide precursor, which may be transformed readily into NKA when activity demands it.<sup>9</sup>

The NMR study reported for NPK in 28% 2,2,2-trifluoroethanol (TFE) shows that NPK adopts a well-defined amphipathic  $\alpha$  helix in its N-terminal half and is relatively disordered in its C-terminal half.<sup>10</sup> CD and NMR studies show that in an aqueous environment NPK lacks a definite secondary structure, although some turn-like elements are present in the N-terminus. The structure is well defined in the presence of dodecylphosphocholine micelles.<sup>11</sup> Extracellular calcium is essential for the action of tachykinins and has been suggested to impose additional structural constraints on the peptides. The calcium-bound conformation of tachykinins has been suggested

Received: July 9, 2012

Published: December 17, 2012

to be required for receptor activation.<sup>12</sup> CD studies on calcium titrations with NPK show that the helicity increases with increasing concentrations of calcium.<sup>11</sup> Data suggest that specific constraints may be imposed on the neuropeptide structure on its interaction with calcium, which may have a role in the bioactive conformation of the peptide and its interaction with the receptor.

The tachykinins, substance P, neurokinin A, neuropeptide K, and neurokinin B were measured in both control (neurologically normal) and Huntington's disease (HD) brains obtained post mortem. All four peptides were significantly reduced in the substantia nigra of Huntington's disease patients compared with the control group.<sup>13</sup> No differences were observed in the frontal or temporal cortex except that neuropeptide K was significantly reduced in the frontal cortex of Huntington's disease cases. Both increased<sup>14</sup> and decreased<sup>15</sup> brain Cu levels have been found in HD patients, compared to the control group. Recently, it has been discovered that cerebrospinal fluid (CSF) free Cu concentration is associated with the clinical stage and time after onset in HD patients.<sup>16</sup>

Almost all living organisms require Fe, Cu, and other transition metals to correctly carry out their most essential metabolic processes. These two redox-active metal ions have the ability to occupy multiple valence states in proteins and most notably activate oxygen used by various enzymes involved in cellular respiration. However, when unregulated, redox-active metals have the ability to react with oxygen to generate reactive oxygen species (ROS) that can be under certain conditions harmful to the organisms and participate in cellular damage at various levels, including proteins, membrane lipids, and DNA.<sup>17,18</sup> An imbalance between the production of ROS and the antioxidant defenses results in the oxidative stress responsible for this damage. In the presence of hydrogen peroxide, ROS are generated by either Haber–Weiss or Fenton reactions.<sup>19–21</sup> In biological milieu, free or bound Cu<sup>2+</sup> could initiate the redox cycle, which is dependent on the thermodynamic properties of the reactants and the structure of the Cu<sup>2+</sup> complexes. For complexes with peptides generation of hydroxyl radicals was observed.<sup>22</sup> It is assumed that H<sub>2</sub>O<sub>2</sub> reduces peptide–Cu<sup>2+</sup> to peptide–Cu<sup>+</sup>; this is followed by reaction of Cu<sup>+</sup> with hydrogen peroxide to give OH·.<sup>23,24</sup> The hydroxyl radical has a very short lifetime (10<sup>–9</sup> s) and is very reactive with practically any biological molecules near the site of its formation.<sup>25</sup> Metal-catalyzed oxidation (MCO) of proteins or peptides is mainly a site-specific process in which only one or a few amino acids at metal-binding sites on the protein are preferentially oxidized.<sup>26–30</sup> All amino acid residues of proteins are susceptible to oxidation by hydroxyl radical ·OH. However, cysteine and methionine residues are particularly sensitive to oxidation by almost all forms of ROS. Under even mild conditions cysteine residues are converted to disulfides and methionine residues are converted to methionine sulfoxide (MeSOX) residues. Most biological systems contain disulfide reductases and MeSOX reductases that can convert the oxidized forms of cysteine and methionine residues back to their unmodified forms. These are the only oxidative modifications of proteins that can be repaired.<sup>31</sup>

The breakdown of copper and other redox metal homeostasis has been described as an important causative factor for various disease states of an organism, including neurological disorders, cancer, cardiovascular disease, as well as other diseases.<sup>32–34</sup>

This study describes the acid–base properties of two fragments: (1-4,18-36)NPK DADS<sup>4</sup>G<sup>18</sup>H<sup>19</sup>GQISH<sup>24</sup>KRH<sup>27</sup>KTDSFVGLM<sup>36</sup>-NH<sub>2</sub> and its acetyl derivative Ac-(1-4,18-36)NPK, Ac-DADS<sup>4</sup>G<sup>18</sup>H<sup>19</sup>GQISH<sup>24</sup>KRH<sup>27</sup>KTDSFVGLM<sup>36</sup>-NH<sub>2</sub> of neuropeptide K (NPK), and their abilities to form the mono- and polynuclear copper(II) complexes. Fragments studied contain all amino acid residues (especially those containing nitrogen donor atoms) of NPK able to bind the copper(II) ions. The N-acetyl fragment was also studied to determine the coordination of the NH<sub>2</sub> terminal group to copper(II) ions. These peptides contain at the N-terminal the sequence DAD<sup>3</sup> and three histidine residues (H<sup>19</sup>, H<sup>24</sup>, H<sup>27</sup>) able to bind the copper(II) ions independently; therefore, the polynuclear complexes were also studied. Copper(II) complexes were studied by the combined application of potentiometric equilibrium and spectroscopic (UV–vis, CD, EPR) and spectrometric (MS) methods. The present paper also presents the products of the copper(II)-catalyzed oxidation on the base of binding sites of the peptides to copper(II) ions at pH 7.4 predicted by potentiometric and spectroscopic methods. We would like to demonstrate the relationship between the binding sites of copper(II) ions and oxidation products according to a site-specific process in which only one or a few amino acids at metal-binding sites on the peptide are preferentially oxidized.<sup>26–30</sup>

## METHODS

**Synthesis of Peptides.** Syntheses of peptides (1-4,18-36)NPK and Ac-(1-4,18-36)NPK were performed on a polystyrene/polyethylene glycol copolymer resin (TentaGel R RAM Resin, substitution 0.18 mmol/g) using Fmoc strategy with continuous-flow methodology (9050 Plus Millipore Peptide Synthesizer).<sup>35–37</sup> Acetylation of the N-terminal amino group was performed on the resin using 1 M acetylimidazole in dimethylformamide (DMF). All peptides were cleaved from the resin and deprotected by 2 h shaking in a mixture containing 94% of trifluoroacetic acid (TFA), 2.5% H<sub>2</sub>O, 2% of triisopropylsilane (TIS), and 1.5% of 1,2-ethanedithiol (EDT).

The resulting crude peptides were purified by reversed-phase high-performance liquid chromatography (RP-HPLC) using a C<sub>8</sub> semi-preparative Phenomenex Luna column (21.2 × 250 mm, 5 μm, 100 Å). As a mobile phase a linear CD gradient was applied, where eluent C was 100 mM aqueous triethylammonium phosphate (TEAP) pH 3.0 ((1-4,18-36)NPK) or 6.8 (Ac-(1-4,18-36)NPK), and eluent D was 26% of acetonitrile (ACN) containing 100 mM TEAP pH 3.0 or 6.8, respectively. The purified peptides were desalted using a linear AB gradient, where (A) 0.1% aqueous TFA and (B) 80% ACN/H<sub>2</sub>O + 0.1% TFA. The peptides were analyzed by analytical reversed-phase high-performance liquid chromatography (RP-HPLC) using a C<sub>8</sub> Kromasil column (4.6 × 250 mm, 5 μm) and a linear gradient 5–100% B completed in 30 min. The peptides' identity was confirmed using matrix-assisted laser desorption/ionization time-of-flight mass spectrometry (MALDI-TOF MS).

Analytical data were as follows. (1-4,18-36)NPK: R<sub>t</sub> = 14.4 min (Kromasil), MS = 2523.3 [M + H]<sup>+</sup>, M<sub>calcd</sub> = 2522.8. Ac-(1-4,18-36)NPK: R<sub>t</sub> = 14.9 min, MS = 2565.9 [M + H]<sup>+</sup>, M<sub>calcd</sub> = 2564.8.

**Potentiometric Measurements.** Stability constants for proton and Cu(II) complexes were calculated from pH-metric titrations, carried out in an argon atmosphere at 298 K using a total volume of 1.5–2 cm<sup>3</sup>. Alkali was added from a 0.250 cm<sup>3</sup> micrometer syringe which was calibrated by both weight titration and titration of standard materials. Experimental details: ligand concentration 1.1 × 10<sup>–3</sup> mol dm<sup>–3</sup>, metal-to-ligand molar ratio 1:1, 2:1, 3:1, and 4:1 for Cu(II):(1-4,18-36)NPK and only 1:1.1 for Cu(II):Ac-(1-4,18-36)NPK because of precipitation at pH 4.5–5 of copper(II) hydroxide or complexes formed for higher metal-to-ligand molar ratios; the ionic strength 0.10 M (KNO<sub>3</sub>); Cu(NO<sub>3</sub>)<sub>2</sub> used as the source of the metal ions; pH-metric titration on a MOLSPIN pH-meter system using a Russell

**Table 1. Formation ( $\log \beta$ ) and Protonation Constants ( $\log K$ ) for the (1-4,18-36)NPK and Ac-(1-4,18-36)NPK Fragments and Comparable Peptides at  $T = 298$  K and  $I = 0.10$  M ( $\text{KNO}_3$ )**

species	(1-4,18-36)NPK	AlloK <sup>a</sup>	1-16H <sup>b</sup>	Ac-(1-4,18-36)NPK	Ac-NPG <sup>c</sup>	HuPrP(84-114) <sup>d</sup>
	$\log \beta$					
HL	11.01 ± 0.07	10.33	9.96	10.87 ± 0.05	10.30	10.68
H <sub>2</sub> L	21.53 ± 0.05	17.96	17.89	21.69 ± 0.03	20.20	20.96
H <sub>3</sub> L	31.16 ± 0.05	24.85	24.84	31.45 ± 0.03	29.19	30.94
H <sub>4</sub> L	38.82 ± 0.05	31.27	31.38	38.55 ± 0.03	36.22	40.22
H <sub>5</sub> L	45.56 ± 0.05	37.07	37.10	45.02 ± 0.03	42.48	46.99
H <sub>6</sub> L	51.84 ± 0.05	40.17	41.47	50.82 ± 0.03	47.83	53.18
H <sub>7</sub> L	57.43 ± 0.05		45.37	54.87 ± 0.03	51.70	58.83
H <sub>8</sub> L	61.32 ± 0.05		48.52	58.21 ± 0.03	54.37	
H <sub>9</sub> L	64.58 ± 0.05		51.18	60.67 ± 0.04		
H <sub>10</sub> L	67.09 ± 0.05					
	$\log K$					
NH <sub>2</sub> -Lys						10.68
NH <sub>2</sub> -Lys						10.29
NH <sub>2</sub> -Lys	11.01			10.87	10.30	9.98
NH <sub>2</sub> -Lys	10.52	10.33	9.96	10.82	9.90	9.28
OH-Ser	9.63			9.76	8.99	
NH <sub>2</sub>	7.66	7.63	7.93			
N-Im	6.74	6.89	6.95	7.10	7.03	6.77
N-Im	6.28	6.42	6.54	6.47	6.26	6.19
N-Im	5.59	5.80	5.72	5.80	5.35	5.64
COO <sup>-</sup>	3.89	3.10	4.37	4.05	3.87	
COO <sup>-</sup>	3.26		3.90	3.34	2.67	
COO <sup>-</sup>	2.51		3.15	2.46		
COO <sup>-</sup>			2.66			

<sup>a</sup>KGVSGHGQHGQVHG (AlloK), ref 66. <sup>b</sup>DAEFRHDSGYEVHHQK-NH<sub>2</sub> (1-16H), ref 67. <sup>c</sup>Ac-DAGHGQISHKRHKTD SFVGLM-NH<sub>2</sub> (Ac-NPG), ref 49. <sup>d</sup>Ac-PHGGGQGGGTHSQWNKPSKPTNMKHMAGA-NH<sub>2</sub>, HuPr(84-114), ref 47.

CMAW 711 semimicro-combined electrode, calibrated in concentration using  $\text{HNO}_3$ ,<sup>38</sup> number of titrations = 2; method of calculation SUPERQUAD<sup>39</sup> and HYPERQUAD.<sup>40</sup> Samples were titrated in the pH region 2.5–10.5. Standard deviations (values) quoted were computed by SUPERQUAD and HYPERQUAD and refer to random errors only. They are, however, a good indication of the importance of the particular species involved in the equilibria.

Titration of the ligand in the presence of various equivalents of copper(II) was analyzed in batch calculations, in which all titration curves are fitted at the same time with one model. Purities and exact concentration of the solutions of the ligand were determined by the method of Gran.<sup>41</sup>

**Spectroscopic Measurements.** Solutions were of similar concentrations to those used in potentiometric studies. Absorption spectra (UV–vis) were recorded on a Cary 50 “Varian” spectrophotometer in the 850–300 nm range. Circular dichroism (CD) spectra were recorded on a Jasco J-715 spectropolarimeter in the 750–250 nm range. Spectra were scanned at pH and stoichiometric M:L values adequate to obtain maximum formation of the particular species, but also in this condition other species coexist at a smaller concentration. Values of  $\Delta \epsilon$  (i.e.,  $\epsilon_L - \epsilon_R$ ) and  $\epsilon$  were calculated at the maximum concentration of the particular species obtained from potentiometric data. Electron paramagnetic resonance (EPR) spectra were performed in an ethylene glycol–water (1:2, v/v) solution at 77 K on a Bruker ESP 300E spectrometer equipped with the ER 035 M Bruker NMR gaussmeter and the HP 5350B Hewlett-Packard microwave frequency counter at the X-band frequency (~9.45 GHz). Spectra were analyzed using Bruker’s WIN-EPR SimFonia software, version 1.25. Copper(II) stock solution was prepared from  $\text{Cu}(\text{NO}_3)_2 \cdot 3 \text{H}_2\text{O}$ . Although potentiometric data calculations for the polynuclear complexes of  $\text{Cu}(\text{II})$ –Ac(1-4,18-36)NPK cannot be made, spectroscopic measurements at pH 10.5 for solutions containing 2:1 and 3:1 metal-to-ligand molar ratios were performed.

**ESI-MS Measurements.** Mass spectra were obtained on a Bruker MicrOTOF-Q spectrometer (Bruker Daltonik, Bremen, Germany)

equipped with an Apollo II electrospray ionization source. The mass spectrometer was operated in positive- or negative-ion mode. Instrumental parameters were as follows: scan range  $m/z$  400–2300, dry gas–nitrogen, temperature 200 °C, reflector voltage 1300 V, detector voltage 1920 V. Samples (1:1, 2:1, 3:1, and 4:1 molar ratios of  $\text{Cu}(\text{II})$ –(1-4,18-36)NPK and 1:1 molar ratio of  $\text{Cu}(\text{II})$ –Ac-(1-4,18-36)NPK at pH about 7) were prepared in water, and pH value was adjusted by addition of concentrated NaOH or  $\text{HNO}_3$  and infused at a flow rate of 3  $\mu\text{L}/\text{min}$ . The instrument was calibrated externally with the Tunemix mixture (Bruker Daltonik, Germany) in quadratic regression mode.

**Materials Used in the Oxidation Process.** Deionized and triply distilled water was used, and the MOPS buffer at pH 7.4 (Sigma-Aldrich, MOPS 3-(*N*-morpholino)propanesulfonic acid)<sup>42</sup> was treated with Chelex 100 resin (sodium form, Sigma-Aldrich) to remove trace metals. Hydrogen peroxide was purchased from Fluka (Perhydrol, 30%); ethylenediaminetetraacetic acid (EDTA) and  $\text{Cu}(\text{NO}_3)_2$  were purchased from POCH. Stock solutions (0.10 M) of EDTA and hydrogen peroxide in MOPS buffer were prepared.

**Oxidation of the Fragments of the Neuropeptide K and N-Acetyl Derivative: Liquid Chromatography–Mass Spectrometry Analysis.** Copper(II)-catalyzed oxidation of the peptide in the presence of hydrogen peroxide was monitored by analytical RP-HPLC on a Varian ProStar 240 station using an XTerra C 18 4.6 × 150 mm column (Waters) at a 30 min linear gradient of 5–100% B, where A used 0.1% aqueous TFA and B used 0.1% TFA in 80% ACN. The reaction mixture (0.2 cm<sup>3</sup>) containing 5 × 10<sup>-4</sup> M peptide and a metal-to-ligand molar ratio of 1:1.1 in a 0.02 M MOPS was incubated at 37 °C for 12h in the presence of hydrogen peroxide at a metal to hydrogen peroxide molar ratio of 1:2 for the (1-4,18-38)NPK and Ac-(1-4,18-36)NPK peptides. The reaction was started by addition of hydrogen peroxide solution, which was freshly prepared. Formation of precipitate after addition of  $\text{H}_2\text{O}_2$  was not observed. After incubation, the reaction was stopped by addition of EDTA to the final complex at an EDTA molar ratio of 1:5. Chelating agent EDTA inhibits oxidation

**Table 2. Stability Constants of Mononuclear Copper(II) Complexes of the (1-4,18-36)NPK and Ac-(1-4,18-36)NPK Fragments and Comparable Peptides at 298 K and  $I = 0.10$  M ( $\text{KNO}_3$ ), and Calculated Deprotonation Constants for Histidine and Amide Protons ( $\text{pK}$ ) in  $\text{Cu(II)}$  Complexes**

species	(1-4,18-36)NPK	AlloK <sup>a</sup>	1-16H <sup>b</sup>	Ac-(1-4,18-36)NPK	Ac-NPG <sup>c</sup>	HuPrP(84-114) <sup>d</sup>
	$\log \beta$					
CuH <sub>6</sub> L	56.00 ± 0.03					57.51
CuH <sub>5</sub> L	51.98 ± 0.01			49.30 ± 0.02	46.31	52.20
CuH <sub>4</sub> L	47.17 ± 0.01	34.95	35.99	44.69 ± 0.01	41.79	46.69
CuH <sub>3</sub> L	40.94 ± 0.02	31.00	31.49	38.80 ± 0.01	36.11	40.13
CuH <sub>2</sub> L	33.90 ± 0.02	26.45	26.22	31.85 ± 0.01	29.60	33.44
CuHL	26.38 ± 0.02	20.30	20.12	24.79 ± 0.01	22.28	25.45
CuL	16.79 ± 0.04	13.37	12.63	16.64 ± 0.01	14.66	16.24
CuH <sub>-1</sub> L		4.89	4.10	6.68 ± 0.01	5.58	6.50
CuH <sub>-2</sub> L		-3.83	-5.21	-4.09 ± 0.01	-3.76	-3.62
CuH <sub>-3</sub> L		-13.28	-15.28		-13.92	-14.62
CuH <sub>-4</sub> L					-24.34	-25.65
pK <sub>1</sub> (His)	4.02	3.95	4.50	4.61	4.52	5.31
pK <sub>2</sub> (His)	4.81	4.55	5.27	5.98	5.68	5.51
pK <sub>3</sub> (His)		6.15				
pK <sub>1</sub> (amide)	7.04	6.93	7.49	6.95	6.51	6.56
pK <sub>2</sub> (amide)	7.52	8.48	8.53	7.06	7.32	6.69
pK <sub>3</sub> (amide)	9.59	8.72	9.31	8.15	7.62	7.99

<sup>a</sup>KGVSGHGQHGQVHG (AlloK), ref 66. <sup>b</sup>DAEFRHDSGYEVHHQK-NH<sub>2</sub> (1-16H), ref 67. <sup>c</sup>Ac-DAGHGQISHKRHKTD SFVGLM-NH<sub>2</sub> (Ac-NPG), ref 49. <sup>d</sup>Ac-PHG GGGWGGGGTSHSQWNKPSKPKTNMKHMAGA-NH<sub>2</sub>, HuPr(84-114), ref 47.

of the peptide by removing Cu(II) from the peptide. Oxidized and digested peptides were desalted on 10  $\mu\text{L}$  ZipTipC18 columns (Omnix, Varian). Columns were prepared by wetting with 50% ACN and equilibrated with 0.1% TFA. Each sample was loaded onto a ZipTip column. The column was washed with 0.1% TFA to remove salts, and then the peptides were eluted with 0.1% formic acid in 80% ACN. Obtained samples were then the subject to LC-ESI-MS analysis. Acetonitrile, water, and formic acid of LC/MS grade were purchased from Sigma. Positive-ion electrospray mass spectrometric analysis was carried out using a Shimadzu ion trap time-of-flight mass spectrometer (LC-MS IT TOF) at unit resolution. Source temperature was 200 °C; electrospray voltage was -1700 V. Separation and mass analysis of oxidized and digested peptides were carried out using a Phenomenex Jupiter Proteo90A analytical column (2 × 150 mm, 4  $\mu\text{m}$ ) with a linear gradient of 0–30% B for 12.5 min followed by a gradient of 30–100% B for 7.5 min (buffer A, 0.2% formic acid/water; buffer B, 0.2% formic acid/ACN; flow rate 0.2 mL/min). Injection volume was 80  $\mu\text{L}$ , and the temperature in which analysis proceeded was 40 °C. Data was acquired and analyzed using LC Solution software provided by Shimadzu.

## RESULTS AND DISCUSSION

**Protonation Constants.** Protonation constants of the (1-4,18-36)NPK and Ac-(1-4,18-36)NPK fragments of neuropeptide K were determined by potentiometric titrations (Table 1). These peptides in the investigated 2.5–10.5 pH range have 10 and 9 protonation sites, respectively. The lysine K<sup>25</sup> and K<sup>28</sup> residues show the highest 11.01–10.52 pK values, in agreement with those reported for other peptides containing this residue.<sup>43–47</sup> The next 9.63–9.76 log  $K$  value, as suggested for neurokinin A,<sup>48</sup> the (1-2,10-21)NPK fragment of neuropeptide gamma,<sup>46</sup> Ac-NPG neuropeptide gamma,<sup>49</sup> and (1-2,7-21)NPK fragment of neuropeptide gamma,<sup>50</sup> may correspond to the protonation constant of the hydroxyl OH group of the serine. It should be mentioned that these peptides contain the same C-terminal sequence, His-Lys-Thr-Asp-Ser-Phe-Val-Gly-Leu-Met-NH<sub>2</sub>. The hallmark of this sequence may be that it contains the so-called “classical” catalytic Ser/His/Asp triad as well the dyads Ser/Lys and Ser/His.<sup>51</sup> Spectroscopic

properties of chymotrypsin and model compounds indicate that a low-barrier hydrogen bond participates in the mechanism of serine protease action.<sup>52</sup> NMR is an important method that has contributed to understanding of the catalytic triad. However, proton NMR studies have largely been limited to the study of the His-H $\delta$ 1 proton because of its shielding from solvent and/or its involvement in a shared hydrogen bond with Asp residue.<sup>53</sup> Chemical exchange saturation transfer (CEST) is a unique nuclear magnetic resonance (NMR) pulse sequence whose ability to detect rapidly exchanging protons has been largely overlooked in biomolecular NMR. CEST provides a potentially useful method for observation of rapidly exchanging amide and hydroxyl protons.<sup>54,55</sup> Using CEST, J. T. Stivers and co-workers<sup>56</sup> observed for the first time the H $\gamma$  proton of Ser<sup>195</sup> at neutral and basic pH values for the S<sub>1</sub> (chymotrypsin, trypsin, thrombin) family of serine proteases. This proton is highly deshielded in the resting enzyme at this pH range due to its hydrogen bond with His<sup>57</sup>-N $\epsilon$ 2, indicating that the Ser<sup>195</sup>-O $\gamma$  is alkoxide-like and preactivated for nucleophilic attack in the free enzyme. In the tachykinin peptides studied<sup>46,48–50</sup> the additional protonation constants (9.00–10.00) were observed, and MS studies suggest deprotonation of a hydroxyl group of Ser residue according to the results obtained from the CEST method. It means that tachykinins containing the C-terminal sequence HKTDSFVGLM-NH<sub>2</sub> with functional groups Asp/Ser/His or Ser/Lys may have in biological systems activities similar to the catalytic triad or dyads of the family serine proteases. Moreover, it should be mentioned that in order to clarify this additional deprotonation in the tachykinins studies of modified neurokinin A (modification Ser/Ala) was performed. Potentiometric data suggest it is most likely that the serine residue in tachykinins studied may be deprotonated. Results for the neurokinin A with point mutation (S5A) are finished and will be published soon.

For the (1-4,18-36)NPK peptide with a free N-terminal amino group, the protonation constant log  $K = 7.66$  (Table 1) corresponds well to protonation of the amino nitrogen, and this

**Table 3. Stability Constants of Polynuclear Copper(II) Complexes of the (1-4,18-36)NPK at 298 K and  $I = 0.10$  M ( $\text{KNO}_3$ ), and Calculated Deprotonation Constants for Histidine and Amide Protons (pK) in Cu(II) Complexes**

species	(1-4,18-36)NPK	species	(1-4,18-36)NPK	species	(1-4,18-36)NPK
			log $\beta$		
$\text{Cu}_2\text{H}_3\text{L}$	$45.07 \pm 0.03$	$\text{Cu}_3\text{L}$	$30.98 \pm 0.08$	$\text{Cu}_4\text{H}_4\text{L}$	$9.84 \pm 0.02$
$\text{Cu}_2\text{H}_2\text{L}$	$39.35 \pm 0.05$	$\text{Cu}_3\text{H}_1\text{L}$	$25.49 \pm 0.02$	$\text{Cu}_4\text{H}_5\text{L}$	$2.26 \pm 0.04$
$\text{Cu}_2\text{HL}$	$33.48 \pm 0.04$	$\text{Cu}_3\text{H}_2\text{L}$		$\text{Cu}_4\text{H}_6\text{L}$	$-5.33 \pm 0.03$
$\text{Cu}_2\text{L}$	$26.76 \pm 0.03$	$\text{Cu}_3\text{H}_3\text{L}$	$11.07 \pm 0.07$	$\text{Cu}_4\text{H}_7\text{L}$	
$\text{Cu}_2\text{H}_{-1}\text{L}$	$19.63 \pm 0.03$	$\text{Cu}_3\text{H}_4\text{L}$	$3.44 \pm 0.03$	$\text{Cu}_4\text{H}_8\text{L}$	$-23.45 \pm 0.03$
$\text{Cu}_2\text{H}_{-2}\text{L}$	$11.43 \pm 0.02$	$\text{Cu}_3\text{H}_5\text{L}$	$-5.32 \pm 0.03$	$\text{Cu}_4\text{H}_9\text{L}$	$-33.61 \pm 0.05$
$\text{Cu}_2\text{H}_{-3}\text{L}$	$1.96 \pm 0.03$	$\text{Cu}_3\text{H}_6\text{L}$		$\text{Cu}_4\text{H}_{10}\text{L}$	$-43.71 \pm 0.03$
$\text{Cu}_2\text{H}_{-4}\text{L}$	$-8.38 \pm 0.04$	$\text{Cu}_3\text{H}_7\text{L}$		$\text{Cu}_4\text{H}_{11}\text{L}$	
$\text{Cu}_2\text{H}_{-5}\text{L}$	$-19.25 \pm 0.06$	$\text{Cu}_3\text{H}_8\text{L}$		$\text{Cu}_4\text{H}_{12}\text{L}$	
$\text{p}K_1(\text{amide})$	5.72	$\text{p}K_4(\text{amide})$	5.49	$\text{p}K_8(\text{amide})$	7.58
$\text{p}K_2(\text{amide})$	5.87	$\text{p}K_5(\text{amide})$	7.21	$\text{p}K_9(\text{amide})$	7.59
$\text{p}K_3(\text{amide})$	6.72	$\text{p}K_6(\text{amide})$	7.21	$\text{p}K_{10}(\text{amide})$	9.06
$\text{p}K_4(\text{amide})$	7.13	$\text{p}K_7(\text{amide})$	7.63	$\text{p}K_{11}(\text{amide})$	9.06
$\text{p}K_5(\text{amide})$	8.20	$\text{p}K_8(\text{amide})$	8.76		
pK	9.47			pK	10.16
pK	10.34			pK	10.10
pK	10.87				

value agrees with those of the peptides containing the aspartic acid residue in the N-terminal position.<sup>49,57,58</sup> For both ligands three log  $K$  values (5.59–7.10, Table 1) fall in the range of basicity of the imidazole ring.<sup>59,60</sup> For both ligands the difference of the three log  $K$  values (around 0.60 log units) is rather small, suggesting that protonation of the histidine residues takes place in overlapping processes. Therefore, these constants are very likely macroconstants containing contributions from protonation of three histidines and cannot be assigned to a specific histidyl residue.

Both peptides studied contain three aspartic acid residues ( $\text{D}^1$ ,  $\text{D}^3$ ,  $\text{D}^{30}$ ), and the log  $K$  values of the protonation of carboxylate functions are found to be in the range 2.46–4.05 (Table 1).<sup>61,62</sup>

**3.2. Copper(II) Complexes of the (1-4,18-36)NPK and Ac-(1-4,18-36)NPK Fragments of Neuropeptide K.** Copper(II)-binding abilities of the (1-4,18-36)NPK and Ac-(1-4,18-36)NPK fragments of neuropeptide K have been studied by combined pH-metric, UV–vis, CD, and EPR spectroscopic, and mass spectrometry (MS) methods at  $[\text{Cu(II)}]:[\text{L}]$  molar ratios 4:1, 3:1, 2:1, and 1:1. Clear aqueous solutions were obtained over the whole 2.5–10.5 pH range studied and metal-to-ligand 1:1, 2:1, 3:1, and 4:1 molar ratios for the (1-4,18-36)NPK fragment, while for the Ac-(1-4,18-36)NPK fragment of neuropeptide K for the 3:1 and 2:1 metal–ligand molar ratios at  $\text{pH} \approx 4.5$ –5 precipitation of most likely the copper(II) hydroxide or complexes was observed. Therefore, calculations of the potentiometric data for the 1:1 Cu(II)–Ac-(1-4,18-36)NPK system were only performed. Tables 2 and 3 contain the formation constants of mononuclear complexes of both ligands studied and polynuclear complexes of the (1-4,18-36)NPK peptide, respectively. Moreover, Tables 2 and 3 also contain the values of the calculated deprotonation constants for amide protons (pK) in Cu(II) complexes. The number of Cu(II) ions that are bonded by the (1-4,18-36)NPK peptide is equal to the number of anchoring sites that are present in the molecule (N-terminal amine and three imidazole nitrogens of His residues). Values of log  $K^*$  of mononuclear complexes, the protonation-corrected stability constants which are useful to compare the ability of various ligands to bind a

metal ion in Tables S1 and S2 (Supporting Information),<sup>63,64</sup> and spectroscopic properties of major complexes in Tables 4 and 5 are given.

Calculations based on the potentiometric data have revealed in the Cu(II)–(1-4,18-36)NPK system the presence of the following species:  $\text{CuH}_6\text{L}$ ,  $\text{CuH}_5\text{L}$ ,  $\text{CuH}_4\text{L}$ ,  $\text{CuH}_3\text{L}$ ,  $\text{CuH}_2\text{L}$ ,  $\text{CuHL}$ , and  $\text{CuL}$  (Table 2, Figure 1, charges omitted for simplicity). Copper(II) ions start binding to the carboxylate group and amine nitrogen atom of the aspartic acid residue  $\text{D}^1$  at pH 3.5 to form the  $\text{CuH}_6\text{L}$  species, as shown in the species distribution diagram (Figure 1).  $\text{CuH}_6\text{L}$  and  $\text{CuH}_5\text{L}$  complexes cannot be characterized by spectroscopic methods because of the very small concentrations and overlap with other species. However, log  $K^*$  values for these species suggest the 1N  $\{\text{NH}_2, \beta\text{-COO}^-\text{Asp}^1\}$  and 2N  $\{\text{NH}_2, \beta\text{-COO}^-\text{Asp}^1, \text{N}_{\text{im}}\}$  coordination modes, respectively (Table S1, Supporting Information). The value of log  $K^*$  for the  $\text{CuH}_6\text{L}$  complex is higher by about 1.2 and 0.69 log units compared to those of  $\text{G}_5\text{H}^{65}$  and  $\text{AlloK}^{66}$ , respectively, but this value is comparable to those of  $\text{DAAA}^{61}$ , 1-10H,<sup>58</sup> 1-16H,<sup>67</sup> and (1-2,10-21)NPG,<sup>46</sup> the peptides containing the aspartic acid residue at the first position of their amino acid sequences ( $\text{D}^1$ ). The stabilization of 1N species results from the bonding of the  $\beta$ -carboxylate oxygen of the  $\text{Asp}^1$  residue in the coordination plane, forming a six-membered chelate ring, and it may suggest the 1N  $\{\text{NH}_2, \beta\text{-COO}^-\text{Asp}^1\}$  coordination mode. With increasing pH, the  $\text{CuH}_5\text{L}$  complex is formed with the pK value for deprotonation of the  $\text{CuH}_6\text{L}$  equal to 4.02 (Table 2), and this value may correspond to deprotonation and coordination of the imidazole nitrogen to the Cu(II) ion.<sup>65,68</sup> Because (1-4,18-36)NPK contains three imidazole nitrogen atoms ( $\text{His}^{19}$ ,  $\text{His}^{24}$ ,  $\text{His}^{27}$ ) and only one of them is coordinated the coordination isomers cannot be excluded.<sup>69</sup> The log  $K^*$  value for the  $\text{CuH}_5\text{L}$  complex is higher by about 1.3 log units in comparison to that of  $\text{G}_5\text{H}$  (–6.76),<sup>65</sup> but it is comparable to those of 1-16H<sup>67</sup> and (1-2,10-21)NPG,<sup>46</sup> supporting coordination of the  $\beta$ -carboxylate group of  $\text{Asp}^1$  in the  $\text{CuH}_5\text{L}$  complex with 2N  $\{\text{NH}_2, \beta\text{-COO}^-\text{Asp}^1, \text{N}_{\text{im}}\}$  binding sites (Table S1, Supporting Information). After deprotonation and coordination of the next imidazole nitrogen to copper(II) ions (pK = 4.81, Table 2) the  $\text{CuH}_4\text{L}$

Table 4. Spectroscopic Data for Mononuclear and Polynuclear Cu(II) Complexes of the (1-4,18-36)NPK Fragment

M:L	species	pH	UV-vis		CD		EPR	
			$\lambda$ [nm]	$\epsilon$ [ $M^{-1} \text{ cm}^{-1}$ ]	$\lambda$ [nm]	$\Delta\epsilon$ [ $M^{-1} \text{ cm}^{-1}$ ]	$A_{\text{II}}$ [G]	$g_{\text{II}}$
1:1	$\text{CuH}_4\text{L}$ , $\text{CuH}_3\text{L}$ , $\{\text{NH}_2, \text{COO}^-, 2\text{N}_{\text{im}}\}$	5.5–6.2	632 <sup>a</sup>	77	758 <sup>a</sup>	0.379	174	2.268
	$\text{CuHL}$ $\{\text{NH}_2, 2\text{N}^-, \text{COO}^-\}$	8.5	548 <sup>a</sup>	121	780 <sup>a</sup>	0.440	210	2.195
2:1	$\text{Cu}_2\text{H}_{-1}\text{L}$ $\{\text{NH}_2, 2\text{N}^-, \text{COO}^-\}$ $\{2\text{N}_{\text{im}}, 2\text{N}^-\}$	7.6	565 <sup>a</sup>	91	758 <sup>a</sup>	-0.186	broad line due to Cu(II)–Cu(II) interactions	
	$\text{Cu}_2\text{H}_{-2}\text{L}$ $\{\text{NH}_2, 2\text{N}^-, \text{COO}^-\}$ $\{\text{N}_{\text{im}}, 3\text{N}^-\}$	8.9	548 <sup>a</sup>	92	614 <sup>a</sup>	-0.317	broad line due to Cu(II)–Cu(II) interactions	
3:1	$\text{Cu}_3\text{H}_{-1}\text{L}$ $\{\text{NH}_2, \text{COO}^-, \text{N}_{\text{im}}\}$ $\{2\text{N}^-, \text{N}_{\text{im}}\}$ $\{2\text{N}^-, \text{N}_{\text{im}}\}$	6.4	560 <sup>a</sup>	95	605 <sup>a</sup>	0.010	broad line due to Cu(II)–Cu(II) interactions	
	$\text{Cu}_3\text{H}_{-5}\text{L}$ $\{\text{NH}_2, 2\text{N}^-, \text{COO}^-\}$ $\{\text{N}_{\text{im}}, 3\text{N}^-\}$ $\{\text{N}_{\text{im}}, 3\text{N}^-\}$	9.5	546 <sup>a</sup>	93	608 <sup>a</sup>	0.295	broad line insignificantly seen in the spectrum with parameters	
4:1	$\text{Cu}_4\text{H}_{-6}\text{L}$ $\{\text{NH}_2, 2\text{N}^-, \text{COO}^-\}$ $\{\text{N}_{\text{im}}, 2\text{N}^-\}$ $\{\text{N}_{\text{im}}, 2\text{N}^-\}$ $\{\text{N}_{\text{im}}, 3\text{N}^-\}$	8.4	558 <sup>a</sup>	92	561 <sup>a</sup>	0.252	very broad line due to Cu(II)–Cu(II) interactions	
	$\text{Cu}_4\text{H}_{-8}\text{L}$ $\{\text{NH}_2, 2\text{N}^-, \text{COO}^-\}$ $\{\text{N}_{\text{im}}, 3\text{N}^-\}$ $\{\text{N}_{\text{im}}, 3\text{N}^-\}$ $\{\text{N}_{\text{im}}, 3\text{N}^-\}$	9.5	553 <sup>a</sup>	92	598 <sup>a</sup>	0.261	very broad line due to Cu(II)–Cu(II) interactions	

<sup>a</sup>d–d transition. <sup>b</sup> $\text{NH}_2 \rightarrow \text{Cu(II)}$  charge transfer transition and  $\text{N}_{\text{im}}(\pi_2) \rightarrow \text{Cu(II)}$  charge transfer transition. <sup>c</sup> $\text{N}_{\text{amide}} \rightarrow \text{Cu(II)}$  charge transfer transition. <sup>d</sup> $\text{N}_{\text{im}} \rightarrow \text{Cu(II)}$  charge transfer transition.

complex is formed in solution in a wide 4.0–7.5 pH range and can be characterized by spectroscopy (Table 4). The EPR parameters  $g_{\text{II}} = 2.268$  and  $A_{\text{II}} = 174 \text{ G}$ <sup>50,67</sup> and d–d transition energy at 632 nm (Figure S1, Supporting Information) may correspond to the  $3\text{N} \{\text{NH}_2, \beta\text{-COO}^-, \text{Asp}^1, 2\text{N}_{\text{im}}\}$  coordination mode. The shift to higher wavelength of the observed  $\lambda_{\text{max}} = 632 \text{ nm}$  compared to that provided by the equation of Prenesti<sup>70</sup> ( $\lambda_{\text{max}} = 604 \text{ nm}$ ) may suggest a distorted geometry

with a significant deviation from planarity around the copper(II) ion by the involvement of the side chain residues of the peptide in an axial interaction (Ser, Asp).<sup>65,71</sup> The  $\log K^*$  value for the  $\text{CuH}_4\text{L}$  complex of the (1-4,18-36)NPK peptide is comparable to those of 1-16H<sup>67</sup> and AlloK<sup>66</sup> (Table S1, Supporting Information), suggesting the  $3\text{N} \{\text{NH}_2, \beta\text{-COO}^-, \text{Asp}^1, 2\text{N}_{\text{im}}\}$  as well as  $3\text{N} \{\text{NH}_2, \text{CO}, 2\text{N}_{\text{im}}\}$  coordination mode. The  $\text{p}K_1(\text{amide})$  value for (1-4,18-36)NPK (7.04, Table 2) is

Table 5. Spectroscopic Data for Cu(II) Complexes of the Ac-(1-4,18-36)NPK Fragment

M:L	species	pH	UV-vis		CD		EPR	
			$\lambda$ [nm]	$\epsilon$ [ $M^{-1} \text{ cm}^{-1}$ ]	$\lambda$ [nm]	$\Delta\epsilon$ [ $M^{-1} \text{ cm}^{-1}$ ]	$A_{II}$ [G]	$g_{II}$
1:1	CuH <sub>4</sub> L {2N <sub>im</sub> }	5.4	654 <sup>a</sup>	56	293 <sup>b</sup>	-0.029	164	2.295
	CuH <sub>3</sub> L {3N <sub>im</sub> }	6.4	618 <sup>a</sup>	75	270 <sup>b</sup>	0.025	180	2.284
	CuHL {2N <sup>-</sup> ,2N <sub>im</sub> }	7.7	575 <sup>a</sup>	84	796 <sup>a</sup>	0.329	171	2.280
					547 <sup>a</sup>	0.099		
					346 <sup>d</sup>	-0.096		
					314 <sup>c</sup>	0.018		
					274 <sup>b</sup>	0.158		
	CuL <sub>2</sub> , CuH <sub>1</sub> L {3N <sup>-</sup> ,N <sub>im</sub> }	9.1	551 <sup>a</sup>	92	620 <sup>a</sup>	0.324	185	2.215
					482 <sup>a</sup>	-0.203		
					355 <sup>d</sup>	-0.059		
					322 <sup>c</sup>	0.233		
					274 <sup>b</sup>	-0.038		
2:1	dinuclear complexes	10.5	544 <sup>a</sup>	88	612 <sup>a</sup>	0.362	215	2.185
					480 <sup>a</sup>	-0.264		
					322 <sup>c</sup>	0.042		
3:1	trinuclear complexes	10.5	551 <sup>a</sup>	90	638 <sup>a</sup>	0.158	215	2.185
					483 <sup>a</sup>	-0.222		
					319 <sup>c</sup>	-0.010		

<sup>a</sup>d-d transition. <sup>b</sup>N<sub>im</sub>( $\pi_2$ )→Cu(II) charge transfer transition. <sup>c</sup>N<sub>amide</sub>→Cu(II) charge transfer transition. <sup>d</sup>N<sub>im</sub>→Cu(II) charge transfer transition.

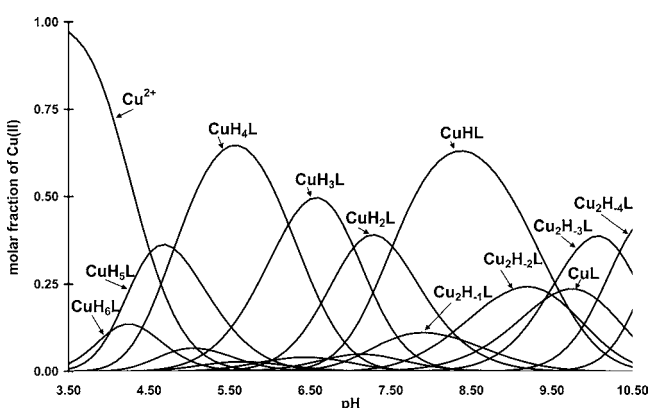


Figure 1. Species distribution of the complexes formed in the copper(II)-(1-4,18-36)NPK system as a function of pH. Cu(II)-to-peptide molar ratio 1:1, [Cu(II)] = 0.001 M.

comparable to those of AlloK (6.93) and 1-16H (7.49), supporting formation of complexes 3N with binding sites {NH<sub>2</sub>, $\beta$ -COO<sup>-</sup>-Asp<sup>1</sup>,2N<sub>im</sub>} or {NH<sub>2</sub>,CO,2N<sub>im</sub>}. The parameters of UV-vis, CD, and EPR spectra are not altered in pH 5.5–6.2, suggesting for the CuH<sub>4</sub>L and CuH<sub>3</sub>L complexes the same 3N binding mode. Moreover, the protonation constant of the CuH<sub>3</sub>L complex (6.23, Table 2) is comparable to that for protonation of the third His residue in the metal-free ligand (6.28, Table 1). Two other species formed by the (1-4,18-36)NPK fragment, i.e., CuH<sub>2</sub>L and CuHL, are complexes with sequential deprotonation and coordination of two amide nitrogens with pK<sub>1</sub>(amide) and pK<sub>2</sub>(amide) of 7.04 and 7.52, respectively (Table 2). The CuHL complex is present in solution in a wide 6.5–10 pH range (Figure 1). For the CuHL complex of (1-4,18-36)NPK the EPR parameters  $A_{II} = 210$  G and  $g_{II} = 2.195$ , the d-d transition energy at 548 nm<sup>72–74</sup> (Figure S1, Supporting Information), and the presence in the CD spectra at 318 nm of the N<sup>-</sup>(amide) → Cu(II) and at 275 nm of the NH<sub>2</sub> → Cu(II) charge transfer transitions strongly support the 3N {NH<sub>2</sub>,2N<sup>-</sup>, $\beta$ -COO<sup>-</sup>-Asp<sup>3</sup>} coordination mode. Values of log K\* for complexes with 3N coordination for the

peptides containing the  $\beta$ -carboxylate group of the Asp residue in the third position are for AADA of -13.02,<sup>72</sup> RKDVY of -9.62,<sup>73</sup> HSDGI-NH<sub>2</sub> of -11.44,<sup>74</sup> and (1-4,18-36)NPK of -12.44 (Table S1, Supporting Information) and suggest a stabilization in the 3N complex compared to pentaalanine amide (-16.44).<sup>75</sup> The abnormal stability of the 3N-coordinated complexes may be the result of the bonding of the  $\beta$ -carboxylate oxygen of the Asp<sup>3</sup> residue in the coordination plane forming a six-membered chelate ring. Aspartic residue in the third position of the peptide sequence stabilizes dramatically the 3N species and prevents coordination of the fourth nitrogen donor.<sup>61,72–74</sup> Deprotonation and coordination of the third amide nitrogen atom occur with pK<sub>3</sub>(amide) = 9.59 (Table 2). However, spectroscopic characterization of this species is impossible because of its very low concentration. As it is seen in Figure 1 for pH > 9.5 in equimolar Cu(II)-(1-4,18-36)NPK solution the dimeric complexes dominate.

The obtained ESI-MS spectra for the Cu(II)-(1-4,18-36)NPK 1:1 metal-to-ligand molar ratio recorded in positive mode show a dominant signal for CuL<sup>2+</sup> ( $m/z$  1293.1 Da), CuHL<sup>3+</sup> ( $m/z$  862.4 Da), and CuH<sub>2</sub>L<sup>4+</sup> ( $m/z$  647.1 Da, Figure 2), supporting formation of the complex in the MS experimental conditions. ESI-MS has been used in a wide variety of fields to study formation, stoichiometry, and speciation of complexes of metals and organic ligands.<sup>76,77</sup>

Potentiometric titration curves reveal that (1-4,18-36)NPK can keep 2, 3, and 4 equiv of copper(II) ions in solution, and precipitation was not observed at any pH values at metal-to-ligand molar ratios of 1:1 and 2:1, 3:1, 4:1. The anchoring sites (amine and three imidazole nitrogen atoms) and binding sites of the peptide are well separated, and the polynuclear complexes can be formed. Then, the copper(II) ions may be coordinated independently from each other by donor atoms of the peptide backbone.<sup>78,79</sup> Figure S2 (Supporting Information) demonstrates the metal ion speciation in the samples at a 2:1 copper(II)-to-ligand molar ratio. It is clear that the dinuclear complexes dominate from pH 5 to 10.5, while the mono- (pH 3.5–5.5) and trinuclear species are also present (pH 5.5–10.5,

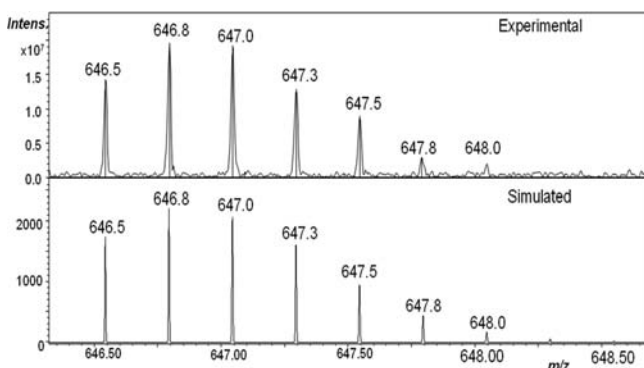


**Figure 2.** ESI mass spectrum for the Cu(II)–(1-4,18-36)NPK system at a 1:1 molar ratio in water solution at pH  $\approx$  7. Experimental and simulated spectra for the  $[\text{CuH}_2\text{L}]^{4+}$  molecular ion with  $m/z$  647.0 Da.

10–25%). For the (1-4,18-36)NPK 2:1 molar ratio the  $\text{Cu}_2\text{H}_{-1}\text{L}$  and  $\text{Cu}_2\text{H}_{-2}\text{L}$  complexes dominate in solution. At pH 7.5–8 (the  $\text{Cu}_2\text{H}_{-1}\text{L}$  complex exists in  $\sim$ 50%) in UV–vis spectra the d–d transition at 565 nm and the presence in the CD spectrum of  $\text{N}_{\text{im}} \rightarrow \text{Cu(II)}$  and  $\text{N}^-(\text{amide}) \rightarrow \text{Cu(II)}$  charge transfer transitions at 348 and 322 nm, respectively, suggest that one metal ion may be coordinated by  $\{\text{NH}_2, 2\text{N}^-, \beta\text{-COO}^-\text{Asp}^3\}$  binding sites and the second Cu(II) ion may be binding by the  $4\text{N}\{\text{N}_{\text{im}}, 2\text{N}^-, \text{N}_{\text{im}}\}$  nitrogen donors. Above pH 7.50, the complex  $\text{Cu}_2\text{H}_{-1}\text{L}$  releases the proton with  $\text{pK}(\text{amide}) = 8.20$  (Table 3). Formation of the  $\text{Cu}_2\text{H}_{-5}\text{LH}_3$  species is accompanied by a significant blue shift of the absorption band to 548 nm (Table 4), suggesting coordination of the additional nitrogen donor and formation in the  $\text{Cu}_2\text{H}_{-2}\text{L}$  complex of  $3\text{N}\{\text{NH}_2, 2\text{N}^-, \beta\text{-COO}^-\text{Asp}^3\}$  and  $4\text{N}\{\text{N}_{\text{im}}, 3\text{N}^-\}$  coordination modes around two copper(II) ions. The parameters of UV–vis, CD, and EPR spectra are not altered at pH 9–10.5, suggesting the coordination mode for the  $\text{Cu}_2\text{H}_{-3}\text{L}$  and  $\text{Cu}_2\text{H}_{-4}\text{L}$  complexes is the same as that for the  $\text{Cu}_2\text{H}_{-2}\text{L}$  species. Moreover, protonation constants of the  $\text{Cu}_2\text{H}_{-5}\text{L}$ ,  $\text{Cu}_2\text{H}_{-4}\text{L}$ , and  $\text{Cu}_2\text{H}_{-3}\text{L}$  complexes (10.87, 10.34, and 9.47, respectively, Table 3) are comparable to those for protonation of two Lys and Ser residues in the metal-free ligand (11.01, 10.52, and 9.63, respectively, Table 1). In order to confirm formation of the polynuclear species the mass spectrometry method was used. For the Cu(II)–(1-4,18-36)NPK 2:1 molar ratio system the dinuclear  $\text{Cu}_2\text{H}_{-2}\text{L}^{2+}$  ( $m/z$  1323.9 Da),  $\text{Cu}_2\text{H}_{-1}\text{L}^{3+}$  ( $m/z$  882.9 Da, Figure 3), and  $\text{Cu}_2\text{HL}^{4+}$  ( $m/z$  666.5 Da) molecular ions were detected in the mass spectra.

As it is seen (Figure S3, Supporting Information), for the 3:1 metal-to-ligand molar ratio mono-, di-, tri-, and tetranuclear complexes are formed. The mononuclear complexes form at low pH (3.5–5.5) range, the dinuclear  $\text{Cu}_2\text{H}_3\text{L}$  species dominates at pH  $\approx$  5, while in higher pH the trimeric  $\text{Cu}_3\text{H}_{-1}\text{L}$  and  $\text{Cu}_3\text{H}_{-5}\text{L}$  complexes are dominant. According to the stoichiometry ( $\text{Cu}_3\text{H}_{-4}\text{LH}_3$ ) and spectroscopic parameters (Table 4) of the UV–vis and CD spectra, the  $\text{Cu}_3\text{H}_{-4}\text{LH}_3$  complex contains metal ions with coordination environments with  $2\text{N}\{\text{NH}_2, \beta\text{-COO}^-\text{Asp}^1, \text{N}_{\text{im}}\}$  and  $2 \times 3\text{N}\{\text{N}_{\text{im}}, 2\text{N}^-\}$  binding mode. The d–d transition energy at 560 nm is consistent with 3N coordination.<sup>43,46</sup> By increasing the pH, the amide nitrogen deprotonation and binding to Cu(II) ions take place, forming the dominant  $\text{Cu}_3\text{H}_{-5}\text{L}$  complex in the pH 8–10.5 range. The blue shift of the d–d transition band with increasing pH to 546 nm (Table 4) suggests coordination of

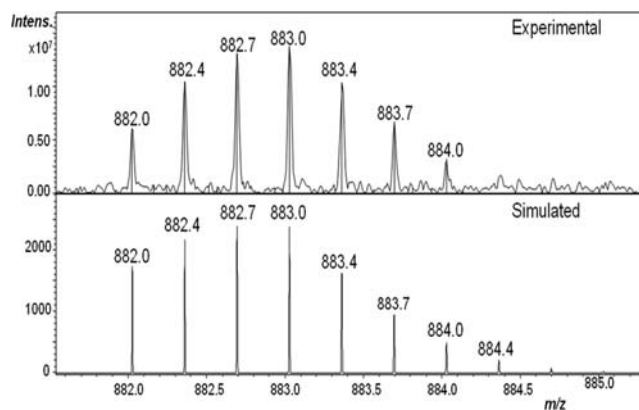


**Figure 3.** ESI mass spectrum for the Cu(II)–(1-4,18-36)NPK system at a 1:1 molar ratio in water solution at pH  $\approx$  7. Experimental and simulated spectra for the  $[\text{Cu}_2\text{H}_{-1}\text{L}]^{3+}$  molecular ion with  $m/z$  882.9 Da.

subsequent nitrogen donors. The  $3\text{N}\{\text{NH}_2, 2\text{N}^-, \beta\text{-COO}^-\text{Asp}^3\}$  and  $2 \times 4\text{N}\{\text{N}_{\text{im}}, 3\text{N}^-\}$  binding sites may be suggested for the  $\text{Cu}_3\text{H}_{-5}\text{L}$  species.

Table 3 and the corresponding speciation curve (Figure 4) reveal that tetranuclear species are also formed in the Cu(II)–

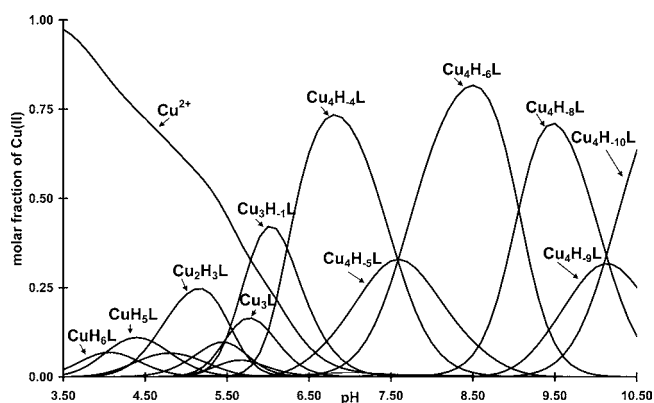


**Figure 4.** Species distribution of the complexes formed in the copper(II)–(1-4,18-36)NPK system as a function of pH. Cu(II)-to-peptide molar ratio 4:1,  $[\text{Cu(II)}] = 0.004\text{ M}$ .

(1-4,18-36)NPK system. As it is seen, the tetranuclear complexes are formed at pH > 6. With increasing pH, the amide nitrogen deprotonations occur and the polynuclear complexes with 3N and 4N binding sites are formed. At pH 9.5 the  $\text{Cu}_4\text{H}_{-11}\text{LH}_3$  complex exists in solution. The d–d transition energy at 553 nm (Table 4) and the stoichiometry strongly suggest the  $3\text{N}\{\text{NH}_2, 2\text{N}^-, \beta\text{-COO}^-\text{Asp}^3\}$  and  $3 \times 4\text{N}\{\text{N}_{\text{im}}, 3\text{N}^-\}$  binding modes around four metal ions (Scheme 1). EPR parameters for the polynuclear complexes (di-, tri-, and tetranuclear) cannot be derived from the spectra because of significant EPR line broadening (Table 4, Figure 5). It suggests some spin–spin interactions between the coordinated Cu(II) ions, indicating that paramagnetic Cu(II) ions are close to each other. The broadening of the EPR line may be due to dipolar as well as exchange interaction between Cu(II) ions.<sup>80</sup> The exchange interaction produces the collapse of the four hyperfine lines, according to the Anderson exchange model.<sup>81</sup> Because the observed line width does not change by increasing or decreasing the concentration (data not shown) this indicates an association of the complexes into larger aggregates leading to



**Scheme 1. Binding Sites of the Copper(II) Ions in the  $\text{Cu}_4\text{H}_{-11}\text{LH}_3$  Complex in the 4:1  $\text{Cu(II)}-(1-4,18-36)\text{NPK}$  System at pH 9.5**

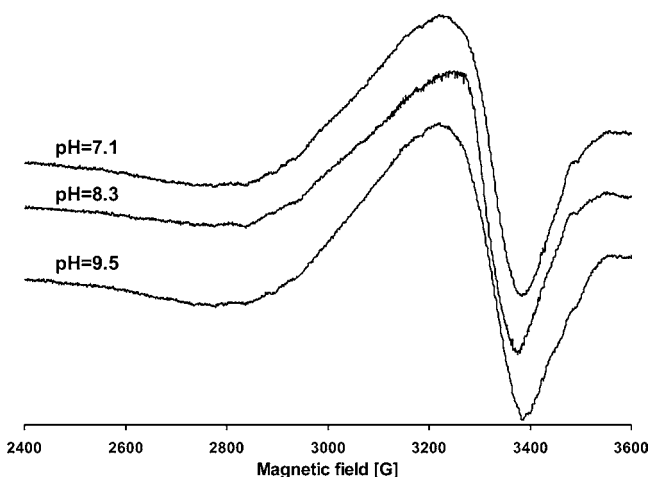
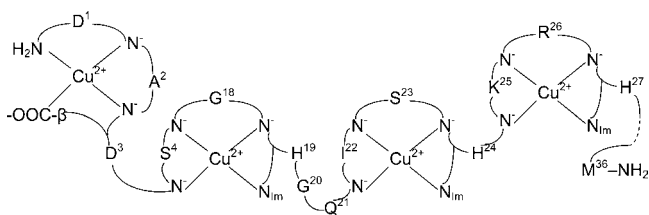


**Figure 5.** Frozen solution EPR spectra of complexes formed in the  $\text{Cu(II)}-(1-4,18-36)\text{NPK}$  fragment 4:1 system at different pH values.

the concentration-independent line broadening by dipolar interactions.<sup>82</sup>

The tri- and tetranuclear copper(II)-(1-4,18-36)NPK complexes were not detected by the MS method. It is most likely that these polynuclear complexes were not stable in the MS experimental conditions.

Protection of the N-terminal group prevents the existence of the coordination modes observed for the neuropeptide (1-4,18-36)NPK, and the anchoring groups are the imidazole nitrogens of the side chains of the H<sup>19</sup>, H<sup>24</sup>, and H<sup>27</sup> histidyl residues. In order to confirm of the coordination of the amine group in  $\text{Cu(II)}-(1-4,18-36)\text{NPK}$ , the  $\text{Cu(II)}-\text{Ac}(1-4,18-36)\text{NPK}$  system was studied. *N*-Acetyl-neuropeptide K,  $\text{Ac}(1-4,18-36)\text{NPK}$  starts coordination of the metal ion at pH 3.5 with formation of the  $\text{CuH}_3\text{L}$  complex in which one of the imidazole nitrogens is deprotonated and coordinated; therefore, coordination isomers may be formed (Figure 6).<sup>69</sup> Although the  $\text{CuH}_5\text{L}$  complex cannot be characterized by spectroscopic methods because of the very small concentrations and overlap with other species, this species can only be characterized by its stoichiometry and formation constants. The value for  $\log K^*$  of  $-1.52$  (Table S2, Supporting Information) is typical for  $1\text{N}\{\text{N}_{\text{im}}\}$  binding sites.<sup>50,83</sup> Four complexes (the  $\text{CuH}_4\text{L}$ ,  $\text{CuH}_3\text{L}$ ,  $\text{CuHL}$ , and  $\text{CuL}$ ) may be characterized by spectroscopy. The parameters of the UV-vis, EPR, and CD measurements of the major species are included in Table 5. The  $\text{pK}$  value for deprotonation of the  $\text{CuH}_3\text{L}$  species equals 4.61 (Table 2). EPR parameters for the  $\text{CuH}_4\text{L}$  complex,  $g_{\text{II}} = 2.295$  and  $A_{\text{II}} = 164$  G, and the absorption band of the d-d transition at 654 nm (Table 5) are consistent with  $2\text{N}\{\text{N}_{\text{im}}, \text{N}_{\text{im}}\}$  coordination of the peptide to copper(II) ions.<sup>67,84,85</sup> The  $\log K^*$  value of the  $\text{CuH}_4\text{L}$  species is quite similar to other two-histidine

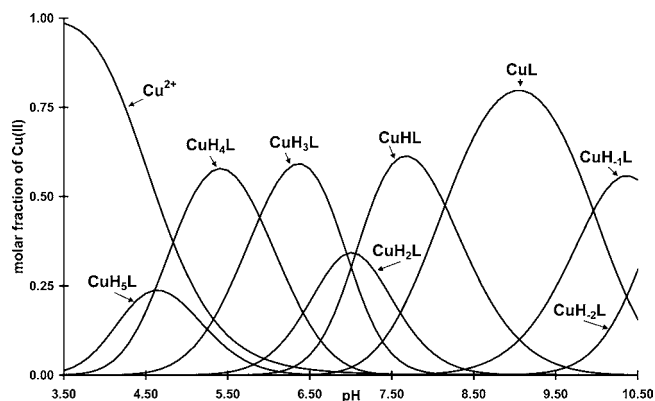


**Figure 6.** Species distribution of the complexes formed in the copper(II)-Ac-(1-4,18-36)NPK system as a function of pH.  $\text{Cu(II)}$ -to-peptide molar ratio 1:1,  $[\text{Cu(II)}] = 0.001$  M.

macrochelates (Table S2, Supporting Information).<sup>67,84–86</sup> By raising the pH the  $\text{CuH}_3\text{L}$  complex is formed with a  $3\text{N}\{3\text{N}_{\text{im}}\}$  binding site. Spectral parameters of this species are in agreement with the equatorial coordination of three imidazole nitrogens.<sup>49,67</sup> It should be mentioned that at the pH where the  $\text{CuH}_4\text{L}$  and  $\text{CuH}_3\text{L}$  complexes exist (maximum concentration) the measurable CD activity of the samples in the range of d-d transitions cannot be recorded (Table 5). It is indirect proof of the coordination of the metal ion by the side chain imidazole residues, which are rather far from the chirality centers of the molecules. With increasing pH the  $\text{CuH}_3\text{L}$  species loses two amide protons with  $\text{pK}_1(\text{amide}) = 6.95$  and  $\text{pK}_2(\text{amide}) = 7.06$  and the  $\text{CuHL}$  complex is formed. EPR parameters  $g_{\text{II}} 2.280$  and  $A_{\text{II}} 171$  G, the d-d transition energy at 575 nm (Table 5), and the presence in CD spectra of  $\text{N}_{\text{im}} \rightarrow \text{Cu(II)}$  at 346 nm and  $\text{N}^-(\text{amide}) \rightarrow \text{Cu(II)}$  at 314 nm charge transfer transitions may suggest the  $4\text{N}\{\text{N}_{\text{im}}, 2\text{N}^-, \text{N}_{\text{im}}\}$  binding mode of the peptide to the metal ion.<sup>87</sup> The cooperative deprotonation of two amide functions (6.95; 7.06) and slightly higher deprotonation of the third amide group (8.15) is promoted by the stability of the  $4\text{N}\{\text{N}_{\text{im}}, 2\text{N}^-, \text{N}_{\text{im}}\}$  complex. Deprotonation and coordination of third amide nitrogen for the peptide studied equals 8.15, while for the Cap43–20aa it equals 6.98.<sup>60</sup> The absorption band of the d-d transition at 551 nm for the  $\text{CuL}$  complex, EPR parameters  $g_{\text{II}} 2.215$  and  $A_{\text{II}} 185$  G, and the presence in the CD spectra at 355 nm of the  $\text{N}_{\text{im}} \rightarrow \text{Cu(II)}$  and 322 nm of the  $\text{N}^-(\text{amide}) \rightarrow \text{Cu(II)}$  charge transfer transitions strongly support the  $4\text{N}\{\text{N}_{\text{im}}, 3\text{N}^-\}$  coordination mode (Table 5). If we compare the predicted  $\lambda_{\text{max}}$  value in the case of a  $\{3\text{N}_{\text{im}}, 3\text{N}^-\}$  coordination mode (522 nm)<sup>88</sup> with the experimental one (551 nm) there is a red shift of 29 nm. This shift may be indicative of an apical coordination of the imidazole.<sup>65,88</sup> Parameters of the UV-vis, EPR, and CD spectra for the  $\text{CuH}_{-1}\text{L}$  complex (to pH 10.5) are similar to those of the  $\text{CuL}$  species, suggesting the same binding mode, and deprotonation of noncoordinated  $\epsilon$ -amino and OH groups of lysine or serine residues occur, respectively.

Mass spectra for the  $\text{Cu(II)}-\text{Ac}(1-4,18-36)\text{NPK}$  1:1 molar ratio solution at  $\text{pH} \approx 7$  revealed the  $[\text{CuL}]^{2+}$  ( $m/z$  1314.2 Da),  $[\text{CuHL}]^{3+}$  ( $m/z$  876.5 Da, Figure 7), and  $[\text{CuH}_2\text{L}]^{4+}$  ( $m/z$  657.6 Da) species. It should be mentioned that for the metal-to-ligand 1:1 molar ratio the dimeric complexes  $[\text{Cu}_2\text{H}_{-2}\text{L}]^{2+}$  ( $m/z$  1344.9 Da),  $[\text{Cu}_2\text{H}_{-1}\text{L}]^{3+}$  ( $m/z$  897.0 Da), and  $[\text{Cu}_2\text{L}]^{4+}$  ( $m/z$  673.0 Da) were also observed, and for the 2:1 and 3:1 metal-

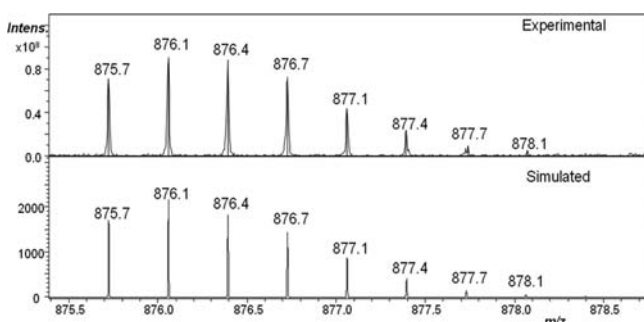


**Figure 7.** ESI mass spectrum for the Cu(II)–Ac-(1-4,18-36)NPK system at a 1:1 molar ratio in water solution at pH  $\approx$  7. Experimental and simulated spectra for the  $[\text{CuHL}]^{3+}$  molecular ion with  $m/z$  876.4 Da.

to-ligand molar ratios only monomeric and dimeric complexes were detected.

Although potentiometric studies for polynuclear complexes of the Cu(II)–Ac-(1-4,18-36)NPK system cannot be performed because of precipitation in the pH 4.5–5.5 range (likely because of hydroxide copper(II) ions), spectroscopic studies at pH 10.5 for the Cu(II)-to-ligand 2:1 and 3:1 molar ratios were carried out (Table 5). EPR parameters  $g_{\text{II}} = 2.185$  and  $A_{\text{II}} = 215$  G and the absorption spectra d–d transition at 544–551 nm strongly support the  $4\text{N} \{N_{\text{im}}, 3\text{N}^-\}$  binding mode of copper(II) ions by the Ac-(1-4,18-36)NPK peptide.<sup>60,67,83,85,86</sup>

**Copper(II)-Catalyzed Oxidation of (1-4,18-36)NPK and Ac-(1-4,18-36)NPK.** It is widely acknowledged that oxidative modification of proteins by reactive oxygen species (ROS) or other reactive substances (RS) is implicated in normal aging and in the etiology or progression of a number of physiological disorders and diseases.<sup>89–91</sup> These reactive species may be generated by a large number of physiological and non-physiological processes,<sup>89</sup> and, nowadays, it is well established that these species are of great importance in the modification of proteins,<sup>92–94</sup> lipids,<sup>95</sup> and nucleic acids.<sup>95,96</sup> Among these biomolecules, proteins are the principal target damage caused by radicals and other oxidants.

Metal-catalyzed oxidation, in which a transition metal ion, reducing agent, and oxygen react to form reactive oxygen species (ROS), is known to occur in vivo and in vitro.<sup>97</sup> In vivo, metals such as Fe(III) and Cu(II) can react with a reducing agent (e.g., flavoprotein, ascorbate, RSH-glutathione) and oxygen to generate ROS such as hydroxyl radical ( $\bullet\text{OH}$ ), hydrogen peroxide ( $\text{H}_2\text{O}_2$ ), and superoxide anion radical ( $\text{O}_2^{\bullet-}$ ), which can ultimately cause damage to proteins.<sup>97,98</sup> The free radical generating Cu(II)–ascorbate and mercaptans– $\text{H}_2\text{O}_2$  systems can be replaced by a Cu(II)– $\text{H}_2\text{O}_2$  system.<sup>99</sup> For Cu(II) complexes with peptides, it is assumed that hydrogen peroxide reduces peptide–Cu(II) to peptide–Cu(I); this is followed by reaction of Cu(I) with hydrogen peroxide to give  $\bullet\text{OH}$ .<sup>24</sup> A unique feature observed during the metal-catalyzed oxidation of proteins is that only a few amino acid residues located in close proximity to each other are modified.<sup>100–102</sup> This site specificity is dependent on the metal-binding site where the reactive oxygen species are generated and also the half-life of reactive oxygen species. The reactive oxygen species are hindered from diffusing into the surrounding medium because they react quickly with amino acid residues near the site of generation.<sup>101,102</sup> The individual amino acids involved in

metal binding to a protein can be conveniently identified through site-specific metal-catalyzed oxidation.<sup>103,104</sup>

Spectroscopic data for the copper(II) complexes of the (1-4,18-36)NPK and Ac-(1-4,18-36)NPK fragments of neuropeptide K in 0.02 M MOPS buffer at 7.4 are similar to those obtained in aqueous solution at pH 7.4 (data not shown, Tables 4 and 5). For the (1-4,18-36)NPK peptide at pH 7.4 the  $\text{CuH}_2\text{L}$  and  $\text{CuHL}$  species are in equilibrium with  $3\text{N} \{ \text{NH}_2, \text{N}^-, \text{CO}, \text{N}_{\text{im}} \}$  and  $3\text{N} \{ \text{NH}_2, 2\text{N}^-, \beta\text{-COO}^-, \text{Asp}^3 \}$  coordination modes, respectively. The Ac-(1-4,18-36)NPK fragment at pH 7.4 forms a dominant  $\text{CuHL}$  complex with  $4\text{N} \{ \text{N}_{\text{im}}, \text{N}^-, \text{N}^-, \text{N}_{\text{im}} \}$  binding mode. Chromatograms of (1-4,18-36)NPK and Ac-(1-4,18-36)NPK after 12 h incubation at 37 °C for the peptide alone, with Cu(II) only, hydrogen peroxide, and with Cu(II)–hydrogen peroxide indicate that the solution containing the copper(II) ions with a 1:1 peptide to copper(II) molar ratio was not changed in comparison to the peptide alone, indicating the lack of oxygen influence on the MCO reaction products.

For the (1-4,18-36)NPK peptide as well as for Ac-(1-4,18-36)NPK after 12 h incubation in 0.02 M MOPS buffer at pH 7.4 oxidation of the methionine residue to methionine sulfoxide was observed (Table 6). Studies on Met oxidation in proteins exposed to oxidant have been reported.<sup>105</sup> Met oxidation can be induced by incubation with oxidizing agents like  $\text{H}_2\text{O}_2$ <sup>106</sup> and is also seen after incubation at elevated temperatures.<sup>107</sup>

Susceptibility of Met residues to oxidation is highly dependent on their solvent exposure and location in the three-dimensional structure of the protein.<sup>107–109</sup> For the systems containing (1-4,18-36)NPK and its acetyl derivative and hydrogen peroxide in a 1:2 molar ratio, after 12 h incubation, LC-MS analysis revealed the presence of mono-oxidized fragments of these peptides. For the 1:2 (1-4,18-36)NPK–hydrogen peroxide system in a chromatographic fraction eluting at 3.1–6 min, a triply and higher charged molecular ions  $[\text{L} + 3\text{H}]^{3+}$ ,  $[\text{L} + 4\text{H}]^{4+}$ , and  $[\text{L} + 5\text{H}]^{5+}$  with  $m/z$  847.4, 635.8, and 508.9 Da are present (Table 6), while for the 1:2 Ac-(1-4,18-36)NPK–hydrogen peroxide system a triply  $[\text{L} + 3\text{H}]^{3+}$  and higher charged molecular ions with  $m/z$  861.4, 646.3, and 517.3 Da are observed in a fraction eluting at 4.6–7.0 min (Table 6). Each of these fragments displayed a molecular mass +16 Da higher than the respective native sequence and may correspond to formation of the methionine sulfoxide. In the presence of hydrogen peroxide and copper(II) ions the peptides underwent oxidation and degradation. Oxidation of methionine provides Met sulfoxide and under extreme conditions sulfone.<sup>110,111</sup> For the Cu(II)–(1-4,18-36)NPK– $\text{H}_2\text{O}_2$  1:1:2 molar ratio system after 12 h incubation in 0.02 M MOPS buffer at pH 7.4 in a chromatographic fraction eluting at 8.2 min,  $[\text{L} + 4\text{H}]^{4+}$  and  $[\text{L} + 5\text{H}]^{5+}$  molecular ions with  $m/z$  640.0 and 512.1 Da are detected (Table 6), while for the Cu(II)–Ac-(1-4,18-36)NPK– $\text{H}_2\text{O}_2$  1:1:2 molar ratio system, the  $[\text{L} + 5\text{H}]^{5+}$  molecular ion with  $m/z$  520.5 Da is observed in a fraction eluting at 3.9 min (Table 6). The molecular masses +32 Da higher than the respective native sequence may correspond to the methionine sulfone. For the Cu(II)–(1-4,18-36)NPK–hydrogen peroxide system with a 1:1:2 molar ratio after 12 h incubation mass spectrometry for the chromatographic fraction eluted at 8.2 min yielded a  $[\text{L} + 5\text{H}]^{5+}$  charged molecular ion of 515.5 Da (Table 6). It may be assigned to the peptide with Met oxidized to sulfone and one histidine residue to 2-oxohistidine, supporting the presence of the histidine residue around the copper(II) ions.<sup>112</sup> Products of

Table 6. Products of Copper(II)-Catalyzed Oxidation of (1-4,18-36)NPK and Ac-(1-4,18-36)NPK Analyzed by LC-MS Spectra

determination of peptide modification	charge	MW <sub>calcd</sub> (Da)	MW <sub>obsd</sub> (Da)	MW <sub>obsd</sub> (Da)
NPK incubation 12 h	3	841.9	$t_R$ (min) = 5.7	842.1
	4	631.7		631.8
	5	505.6		505.7
oxidation of Met → sulfoxide	4	635.7	635.8	
	5	508.8	508.9	
NPK + H <sub>2</sub> O <sub>2</sub> (1:2) incubation 12 h			$t_R$ (min) = 3.1–6.0	
oxidation of Met → sulfoxide	3	847.3		847.4
	4	635.7		635.8
	5	508.8		508.9
Cu(II)–NPK + H <sub>2</sub> O <sub>2</sub> (1:1:2) incubation 12 h			$t_R$ (min) = 3.3	$t_R$ (min) = 8.2
oxidation of Met → sulfone	4	639.7		640.0
	5	512.0		512.1
oxidation of Met → sulfone and His → 2-oxo-His	4	515.2		515.5
loss of CH <sub>3</sub> SOH fragment from peptide	5	496.0		496.7
loss of CH <sub>3</sub> SOH fragment from peptide and oxidation of His → 2-oxo-His	4	626.7		627.3
	5	502.4		502.3
cleavage of A <sup>2</sup> –D <sup>3</sup> peptide bond by $\alpha$ -amidation (D <sup>3</sup> –M <sup>36</sup> ) fragment and oxidation of Met → sulfoxide	4	589.2	589.3	
	5	471.5	471.6	
cleavage of A <sup>2</sup> –D <sup>3</sup> peptide bond by $\alpha$ -amidation (D <sup>3</sup> –M <sup>36</sup> ) fragment and decarboxylation of D to pyruvate on peptide and Met → sulfoxide and His → 2-oxo-His or Met → Sulfone	5	462.7	462.8	
cleavage of D <sup>3</sup> –S <sup>4</sup> peptide bond by $\alpha$ -amidation (S <sup>4</sup> –M <sup>36</sup> ) fragment and oxidation of Met → sulfoxide	4	560.4	560.5	
Ac-NPK incubation 12 h			$t_R$ (min) = 5.7	$t_R$ (min) = 7.0
oxidation of Met → sulfoxide	3	855.9		856.1
	4	642.2		642.4
	5	514.0		514.1
oxidation of Met → sulfoxide	4	646.2	646.4	
	5	517.2	517.3	
Ac-NPK + H <sub>2</sub> O <sub>2</sub> (1:2) incubation 12 h			$t_R$ (min) = 4.6–7.0	
oxidation of Met → sulfoxide	3	861.3		861.4
	4	646.2		646.3
	5	517.2		517.3
Cu(II)–Ac-NPK + H <sub>2</sub> O <sub>2</sub> (1:1:2) incubation 12 h			$t_R$ (min) = 3.9	
oxidation of Met → sulfone	5	520.4		520.5
cleavage of D <sup>1</sup> –A <sup>2</sup> peptide bond by $\alpha$ -amidation (A <sup>2</sup> –M <sup>36</sup> ) fragment and oxidation of Met → sulfoxide	4	606.9		607.1
	5	485.7		485.9
	4	618.9		617.6
cleavage of D <sup>1</sup> –A <sup>2</sup> peptide bond by $\alpha$ -amidation (A <sup>2</sup> –M <sup>36</sup> ) fragment and oxidation of Met → sulfone and two His → 2-oxo-His	5	495.3		494.3
	4	589.2		588.8
cleavage of A <sup>2</sup> –D <sup>3</sup> peptide bond by $\alpha$ -amidation (D <sup>3</sup> –M <sup>36</sup> ) fragment and oxidation of Met → sulfoxide	5	471.5		471.3
	5	480.4		479.9
cleavage of A <sup>2</sup> –D <sup>3</sup> peptide bond by $\alpha$ -amidation (D <sup>3</sup> –M <sup>36</sup> ) fragment and decarboxylation of D to pyruvate on peptide and Met → sulfoxide and His → 2-oxo-His or Met → sulfoxide	5	480.4		479.9
cleavage of A <sup>2</sup> –D <sup>3</sup> peptide bond by $\alpha$ -amidation (D <sup>3</sup> –M <sup>36</sup> ) fragment and loss of CH <sub>3</sub> SOH fragment from peptide and oxidation of one His → 2-oxo-His and one His → Asp	5	457.5		457.0

oxidation formed by characteristic loss of the CH<sub>3</sub>SOH group were identified for peptides containing the methionine residue.<sup>113</sup> In the MS spectrum the peak corresponding to a loss of 64 Da (CH<sub>3</sub>SOH) is diagnostic for methionine sulfoxide.<sup>103</sup> After 12 h incubation of the Cu(II)–(1-4,18-36)NPK–hydrogen peroxide 1:1:2 system the peptide with loss of CH<sub>3</sub>SOH was observed (Table 6). The coordination 3N {NH<sub>2</sub>, 2N<sup>−</sup>,  $\beta$ -COO<sup>−</sup>-Asp<sup>3</sup>} of the (1-4,18-36)NPK peptide at pH 7.4 to copper(II) ions suggests fragmentation by cleavage of the peptide bonds near the D<sup>1</sup>–A<sup>2</sup>–D<sup>3</sup>–S<sup>4</sup>– residues. After 12 h incubation, LC-MS analysis revealed the presence of the D<sup>3</sup>–M<sup>36</sup> fragment with oxidized Met residue. In a chromatographic

fraction eluting at 3.3 min, [L + 4H]<sup>4+</sup> and [L + 5H]<sup>5+</sup> charged molecular ions with  $m/z$  589.3 and 471.6 Da, respectively, were observed.

For oxidation of the Cu(II)–Ac(1-4,18-36)NPK system in the presence of hydrogen peroxide, the 1:2 complex–H<sub>2</sub>O<sub>2</sub> molar ratio was also used, and further oxidations of the methionine and histidine residues were observed (Table 6). Fragmentations of the peptide by cleavage of the peptide bonds D<sup>1</sup>–A<sup>2</sup>, A<sup>2</sup>–D<sup>3</sup> near the His<sup>19</sup> residue may suggest the presence of these amino acids (A, D, H) near the binding site of copper(II) ions. In a chromatographic fraction eluting at 3.9 min, [L + 4H]<sup>4+</sup> and [L + 5H]<sup>5+</sup> charged molecular ions with

$m/z$  617.6 and 494.3 Da, respectively, are present, which may correspond to the  $A^2-M^{36}$  fragment with oxidation of Met to sulfone and two His residues to 2-oxohistidines (Table 6, Figure 8). At pH 7.4 the CuHL complex exists in solution with

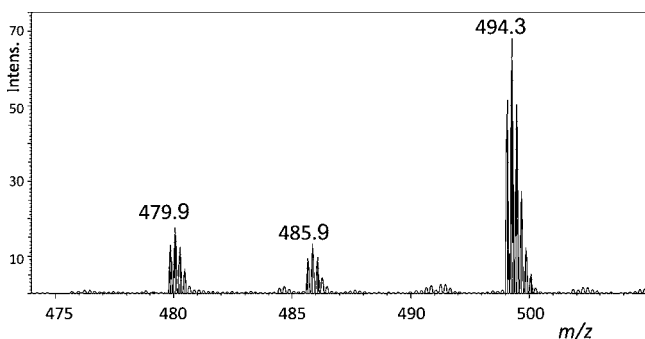


**Figure 8.** MS spectrum of the chromatographic fraction eluting at a retention time of 3.9 min of the Ac-(1-4,18-36) fragment after Cu(II)-catalyzed oxidation. Peptide modifications for the  $[L + 5H]^{5+}$  molecular ions are given in Table 6.

a  $4N \{N_{Im}, N^-, N^-, N_{Im}\}$  binding mode; therefore, oxidation of two histidine residues may be observed. Cleavage of the peptide bonds near the His<sup>19</sup> may suggest that this residue may be coordinated to the copper(II) ions.

#### 4. CONCLUSIONS

The (1-4,18-36)NPK fragment contains main binding sites of neuropeptide K (especially amino acid residues containing nitrogen donor atoms). In the part 4-18 amino acids sequence there are not principal binding sites of this peptide to copper(II) ions (especially the nitrogen atom donors). Fragments studied here contain three histidine residues (H<sup>19</sup>, H<sup>24</sup>, H<sup>27</sup>). For the Ac-(1-4,18-36)NPK fragment the imidazole nitrogen of the histidine residue acts as an anchoring bonding site. In pH range 7.0–8.3 the CuHL complex dominates in solution with  $4N \{N_{Im}, N^-, N^-, N_{Im}\}$  coordination to the metal ions. At pH > 8.3 the major complex with  $4N \{N_{Im}, 3N^-\}$  binding site is present. The presence of the N-terminal amino group has a major influence on both the speciation and the structures of the complexes formed. The N-terminal amino group takes part in the coordination of the copper(II) ions. Coordination of the metal ions likely starts from the amine group with formation of the CuH<sub>6</sub>L complex with  $1N \{NH_2, \beta-COO^-, Asp^1\}$  binding site. With increasing pH the CuH<sub>4</sub>L and CuHL complexes dominate. In wide pH range 4–7 the CuH<sub>4</sub>L complex exists in solution with  $3N \{NH_2, \beta-COO^-, Asp^1, 2N_{Im}\}$  coordination mode, while at pH 7–10 the CuHL species with  $3N \{NH_2, 2N^-, \beta-COO^-, Asp^3\}$  binding site exists. For the Cu(II)–(1-4,18-36)NPK 2:1 molar ratio system only the Cu<sub>2</sub>H<sub>2</sub>L complex with maximum 50% molar fraction of copper(II) ions is present at pH 7–10 with  $3N \{NH_2, 2N^-, \beta-COO^-, Asp^3\}$  and  $4N \{N_{Im}, 3N^-\}$  coordination mode, while the others are present with less than 50% molar fraction. For a 3:1 metal-to-ligand molar ratio the Cu<sub>3</sub>H<sub>1</sub>L (Cu<sub>3</sub>H<sub>4</sub>L H<sub>3</sub>) complex with the  $2N \{NH_2, \beta-COO^-, Asp^1, N_{Im}\} 3N \{N_{Im}, 2N^-\} 3N \{N_{Im}, 2N^-\}$  at pH range 5.5–7.5 and 7.5–10.5 complex Cu<sub>3</sub>H<sub>5</sub>L (Cu<sub>3</sub>H<sub>8</sub>LH<sub>3</sub>) with the  $3N \{NH_2, 2N^-, \beta-COO^-, Asp^3\} 4N \{N_{Im}, 3N^-\} 4N \{N_{Im}, 3N^-\}$  coordination mode dominate. For the Cu(II)–(1-4,18-36)NPK 4:1 system at pH > 6 three complexes dominate, the Cu<sub>4</sub>H<sub>4</sub>L (Cu<sub>3</sub>H<sub>7</sub>LH<sub>3</sub>), Cu<sub>4</sub>H<sub>6</sub>L (Cu<sub>3</sub>H<sub>9</sub>LH<sub>3</sub>), and Cu<sub>4</sub>H<sub>8</sub>L (Cu<sub>3</sub>H<sub>11</sub>LH<sub>3</sub>), where

deprotonation and coordination of sequential amide nitrogen atoms occur.

Oxidation of methionine plays an important role in vivo during biological conditions of oxidative stress, as well as for protein stability in vitro. Modification of methionine to methionine sulfoxide (MetO) can be repaired by methionine sulfoxide reductase (Msr), which catalyzes the thioredoxin-dependent reduction of MetO back to methionine both in vitro<sup>114</sup> and in vivo.<sup>115</sup> The individual amino acids involved in metal binding to a protein can be conveniently identified through site-specific metal-catalyzed oxidation.<sup>101</sup> For both fragments of neuropeptide K, the methionine residue is converted to methionine sulfoxide in the presence of and without hydrogen peroxide, while for the 1:1:2 Cu(II)–peptide–hydrogen peroxide system oxidations of the histidine residue to 2-oxo-histidine and methionine sulfoxide to sulfone were observed. For the Cu(II)–peptide–H<sub>2</sub>O<sub>2</sub> system, a loss of sulfonic acid (CH<sub>3</sub>SOH) from the oxidized methionine (M<sup>36</sup>) residue was detected. Under the experimental conditions for both fragments of neuropeptide K fragmentation by cleavage of the D<sup>1</sup>–A<sup>2</sup>, A<sup>2</sup>–D<sup>3</sup>, and D<sup>3</sup>–S<sup>4</sup> peptide bonds is observed, indicating the involvement of the N-terminal part of the peptides in the copper(II)-binding sites.

#### ■ ASSOCIATED CONTENT

##### Supporting Information

UV–vis spectra of Cu(II)–(1-4,18-36)NPK 1:1 system at different pH; species distribution of the complexes formed in the copper(II)–(1-4,18-36)NPK system as a function of pH and metal-to-ligand 2:1; 3:1 molar ratios; calculated log  $K^*$  for the mononuclear Cu(II) complexes of the (1-4,18-36)NPK fragment and comparable ligands at  $T = 298$  K and  $I = 0.10$  M (KNO<sub>3</sub>); calculated log  $K^*$  for the mononuclear Cu(II) complexes of Ac-(1-4,18-36)NPK fragment and comparable ligands at  $T = 298$  K and  $I = 0.10$  M (KNO<sub>3</sub>). This material is available free of charge via the Internet at <http://pubs.acs.org>.

#### ■ AUTHOR INFORMATION

##### Corresponding Author

\*Phone: (048)(71)375-72-31. Fax: (048) (71) 328-23-48. E-mail: [teresa.kowalik-jankowska@chem.uni.wroc.pl](mailto:teresa.kowalik-jankowska@chem.uni.wroc.pl).

##### Notes

The authors declare no competing financial interest.

#### ■ ACKNOWLEDGMENTS

Financial support from the Polish State Committee for Scientific Research KBN Grant NN204 249534 and the European Social Fund is gratefully acknowledged.

#### ■ REFERENCES

- (1) Tatemoto, K.; Lundberg, J. M.; Jornvall, H.; Mutt, V. *Biochem. Biophys. Res. Commun.* **1985**, *128*, 947–953.
- (2) Arai, H.; Emson, P. C. *Brain Res.* **1986**, *399*, 240–249.
- (3) Valentino, K. L.; Tatemoto, K.; Hunter, J.; Barchas, J. D. *Peptides* **1986**, *7*, 1043–1059.
- (4) Nakanishi, S. *Physiol. Rev.* **1987**, *67*, 1117–1142.
- (5) Harmar, A. J.; Armstrong, A.; Pascal, J. C.; Chapman, K.; Rosie, R.; Curtis, A.; Goings, J.; Edwards, C. R. W.; Fink, G. *FEBS Lett.* **1986**, *208*, 67–72.
- (6) Krause, J. E.; Chirgwin, J. M.; Carter, M. S.; Xu, Z. S.; Hershey, A. D. *Proc. Natl. Acad. Sci. U.S.A.* **1987**, *84*, 881–885.
- (7) Mori, M.; Yokota, Y.; Yasue, M.; Serikawa, T.; Yamada, J. *Cytogenet. Cell Genet.* **1992**, *60*, 222–223.

- (8) Decarie, A.; Couture, R. *Eur. J. Pharmacol.* **1992**, *213*, 125–131.
- (9) Diez-Guerra, F. J.; Richardson, P. J.; Emson, P. C. *J. Neurochem.* **1988**, *50*, 440–450.
- (10) Horne, J.; Sadek, M.; Craik, D. J. *Biochemistry* **1993**, *32*, 7406–7412.
- (11) Dike, A.; Owsik, S. M. *Biochemistry* **2006**, *45*, 2994–3004.
- (12) Ananthanarayanan, V. S.; Orlicy, S. *Biopolymers* **1992**, *32*, 1765–1773.
- (13) Arai, H. M. D.; Emson, P. C.; Carrasco, L. H. M. D. *Ann. Neurol.* **1987**, *22*, 587–594.
- (14) Dexter, D. T.; Jenner, P.; Schapira, A. H.; Marsden, C. D. *Ann. Neurol.* **1992**, *32* (Suppl), S94–100.
- (15) Loeffler, D. A.; Le Witt, P. A.; Juneau, P. L.; Sima, A. A.; Nguyen, H. U.; De Maggio, A. J.; Brickman, C. M.; Brewer, G. J.; Dick, R. D.; Triyer, M. D.; Kanaley, L. *Brain Res.* **1996**, *738*, 265–274.
- (16) Boll, M. C.; Alcaraz-Zubeldia, M.; Montes, S.; Rios, C. *Neurochem. Res.* **2008**, *33*, 1717–1723.
- (17) Valko, M.; Morris, H.; Cronin, M. T. D. *Curr. Med. Chem.* **2005**, *12*, 1161–1208.
- (18) Jamova, K.; Baros, S.; Valko, M. *Transition Met. Chem.* **2012**, *37*, 127–134.
- (19) Haliwell, B.; Gutteridge, J. M. *Methods Enzymol.* **1990**, *186*, 1–85.
- (20) Baruch-Suchodolsky, R.; Fischer, B. *Biochemistry* **2009**, *48*, 4354–4370.
- (21) Koppenol, W. H. *Redox Rep.* **2001**, *6*, 229–234.
- (22) Ueda, J.-I.; Shimazu, Y.; Ozawa, T. *Biochem. Mol. Biol. Int.* **1994**, *34*, 801–808.
- (23) Simpson, J. A.; Cheeseman, K. H.; Smith, S. E.; Dean, R. T. *Biochem. J.* **1988**, *254*, 519–523.
- (24) Ozawa, T.; Hanaki, A. J. *J. Chem. Soc., Chem. Commun.* **1991**, 330–332.
- (25) Cadet, J.; Douki, T.; Ravanat, J. L. *Mutat. Res.* **2011**, *711*, 3–12.
- (26) Stadtman, E. R.; Berlett, B. S. *Chem. Res. Toxicol.* **1997**, *10*, 485–494.
- (27) Uchida, K.; Kawakishi, S. *J. Biol. Chem.* **1994**, *269*, 2405–2410.
- (28) Hawkins, C. L.; Davies, M. J. *Biochim. Biophys. Acta* **1997**, *1360*, 84–96.
- (29) Cheng, R. Z.; Kawakishi, S. *Eur. J. Biochem.* **1994**, *223*, 759–764.
- (30) Li, S.; Nguyen, T. H.; Schoneich, Ch; Borhardt, R. T. *Biochemistry* **1995**, *34*, 5762–5772.
- (31) Berlett, B. S.; Stadtman, E. R. *J. Biol. Chem.* **1997**, *272*, 20313–20316.
- (32) Truscott, R. J. *Exp. Eye Res.* **2005**, *80*, 709–725.
- (33) Gaggelli, E.; Kozłowski, H.; Valensin, D.; Valensin, G. *Chem. Rev.* **2006**, *106*, 1995–2044.
- (34) Rivera-Mancia, S.; Perez-Neri, I.; Rios, C.; Tristan-Lopez, L.; Rivera-Espinosa, L.; Montes, S. *Chem.-Biol. Interact.* **2010**, *186*, 184–199.
- (35) Steward, J. M.; Young, J. D. *Solid Phase Peptide Synthesis*; Pierce Chemical Co.: Rockford, IL, 1993.
- (36) *Millipore 9050 Plus PepSynthesizer Operator's Guide*; Millipore Corp.: Milford, 1992.
- (37) Sole, N.; Barany, G. *J. Org. Chem.* **1992**, *57*, 5399–5403.
- (38) Irving, H.; Miles, M. G.; Pettit, L. D. *Anal. Chim. Acta* **1967**, *38*, 475–488.
- (39) Gans, G.; Sabatini, A.; Vacca, A. *J. Chem. Soc., Dalton Trans.* **1985**, 1195–1199.
- (40) Gans, G.; Sabatini, A.; Vacca, A. *Talanta* **1996**, *43*, 1739–1753.
- (41) Gran, G. *Acta Chem. Scand.* **1950**, *4*, 559–577.
- (42) Good, N. E.; Winget, G. D.; Winter, W.; Connolly, T. N.; Izawa, S.; Singh, R. M. M. *Biochemistry* **1966**, *5*, 467–477.
- (43) Zavitsanos, K.; Nunes, A. M. P. C.; Malandrinos, G.; Kallay, C.; Sovago, I.; Magafa, V.; Cordopatis, P.; Hadjiladis, N. *Dalton Trans.* **2008**, 6179–6187.
- (44) La Mendola, D.; Magri, A.; Hansson, O.; Bonomo, R. P.; Rizzarelli, E. *J. Inorg. Biochem.* **2009**, *103*, 758–765.
- (45) Kowalik-Jankowska, T.; Rajewska, A.; Jankowska, E.; Grzonka, Z. *Dalton Trans.* **2007**, 4197–4206.
- (46) Kowalik-Jankowska, T.; Jankowska, E.; Kasprzykowski, F. *Inorg. Chem.* **2010**, *49*, 2182–2192.
- (47) Osz, K.; Nagy, Z.; Pappalardo, G.; Di Natale, G.; Sanna, D.; Micera, G.; Rizzarelli, E.; Sovago, I. *Chem.—Eur. J.* **2007**, *13*, 7129–7143.
- (48) Kowalik-Jankowska, T.; Jankowska, E.; Szewczuk, Z.; Kasprzykowski, F. *J. Inorg. Biochem.* **2010**, *104*, 831–842.
- (49) Pietruszka, M.; Jankowska, E.; Kowalik-Jankowska, T.; Szewczuk, Z.; Smużyńska, M. *Inorg. Chem.* **2011**, *50*, 7489–7499.
- (50) Jankowska, E.; Pietruszka, M.; Kowalik-Jankowska, T. *Dalton Trans.* **2012**, *41*, 1683–1694.
- (51) Kici, O. D.; Paetzel, M.; Dalby, R. E. *Protein Sci.* **2008**, *17*, 2023–2037.
- (52) Frey, A. P.; Whitt, S. A.; Tobie, J. B. *Science* **1994**, *264*, 1927–1930.
- (53) Bachovchin, W. *Magn. Reson. Chem.* **2001**, *39*, S199–S213.
- (54) Mc Mahon, M. T.; Gilad, A. A.; Zhou, J.; Sun, P. Z.; Bulte, J. W. M.; van Zijl, P. *Magn. Reson. Med.* **2006**, *55*, 836–847.
- (55) Mc Mahon, M. T.; Gilad, A. A.; Deliso, M. A.; Berman, S. M.; Bulte, J. M.; van Zijl, P. C. *Magn. Reson. Med.* **2008**, *60*, 803–812.
- (56) Lauzon, C. B.; van Zijl, P.; Stivers, J. T. *J. Biomol. NMR* **2011**, *50*, 299–314.
- (57) Damante, Ch.A.; Osz, K.; Nagy, Z.; Pappalardo, G.; Grasso, G.; Impellizzeri, G.; Rizzarelli, E.; Sovago, I. *Inorg. Chem.* **2008**, *47*, 9669–9683.
- (58) Kowalik-Jankowska, T.; Ruta-Dolejsz, M.; Wisniewska, K.; Lankiewicz, L. *J. Inorg. Biochem.* **2001**, *86*, 535–545.
- (59) La Mendola, D.; Farkas, D.; Bellia, F.; Magri, A.; Travaglia, A.; Hansson, O.; Rizzarelli, E. *Inorg. Chem.* **2012**, *51*, 128–141.
- (60) Zorrodo, M. A.; Kowalik-Jankowska, T.; Medici, S.; Peana, M.; Kozłowski, H. *Dalton Trans.* **2008**, 6127–6134.
- (61) Galey, J. F.; Decock-Le Reverend, B.; Lebkiri, A.; Pettit, L. D.; Pyburn, S. I.; Kozłowski, H. *J. Chem. Soc.; Dalton Trans.* **1991**, 2281–2287.
- (62) Kallay, C.; Nagy, Z.; Varnagy, K.; Malandrinos, G.; Hadjiladis, N.; Sovago, I. *J. Bioinorg. Chem. Appl.* **2007**, 1–9, DOI: 10.1155/2007/30394.
- (63) Kozłowski, H.; Bal, W.; Dyba, M.; Kowalik-Jankowska, T. *Coord. Chem. Rev.* **1999**, *183*, 319–346.
- (64) Bal, W.; Dyba, M.; Kasprzykowski, F.; Kozłowski, H.; Latajka, R.; Lankiewicz, L.; Mackiewicz, Z.; Pettit, L. D. *Inorg. Chim. Acta* **1998**, *283*, 1–11.
- (65) Varnagy, K.; Szabo, J.; Sovago, I.; Malandrinos, G.; Hadjiladis, N.; Sanna, D.; Micera, G. *Dalton Trans.* **2000**, 467–472.
- (66) Kuczer, M.; Pietruszka, M.; Kowalik-Jankowska, T. *J. Inorg. Biochem.* **2012**, *111*, 40–49.
- (67) Kowalik-Jankowska, T.; Ruta, M.; Wisniewska, K.; Lankiewicz, L. *J. Inorg. Biochem.* **2003**, *95*, 270–282.
- (68) Gyurcsik, B.; Vosekalna, I.; Larsen, E. *Acta Chem. Scand.* **1997**, *51*, 49–58.
- (69) Timari, S.; Kallay, C.; Osz, K.; Sovago, I.; Varnagy, K. *Dalton Trans.* **2009**, 1962–1971.
- (70) Prenesti, E.; Daniele, P. G.; Prencipe, M.; Ostacoli, G. *Polyhedron* **1999**, *18*, 3233–3241.
- (71) Kallay, C.; Turi, I.; Timari, S.; Nagy, Z.; Sanna, D.; Pappalardo, G.; De Bona, P.; Rizzarelli, E.; Sovago, I. *Maonatsh. Chem.* **2011**, *142*, 411–419.
- (72) Decock-Le Reverend, B.; Lebkiri, A.; Livera, C.; Pettit, L. D. *Inorg. Chim. Acta* **1986**, *124*, L19–L22.
- (73) Sovago, I.; Kiss, T.; Gergely, A. *Inorg. Chim. Acta* **1984**, *93*, L53–L55.
- (74) Kowalik-Jankowska, T.; Jasionowski, M.; Lankiewicz, L. *J. Inorg. Biochem.* **1999**, *76*, 63–70.
- (75) Bal, W.; Kozłowski, H.; Kupryszewski, G.; Mackiewicz, Z.; Pettit, L. D.; Robbins, R. *J. Inorg. Biochem.* **1993**, *52*, 79–87.
- (76) Keith-Roach, M. *Anal. Chim. Acta* **2010**, *678*, 140–148.
- (77) Moini, M. *Rapid Commun. Mass Spectrom.* **2010**, *24*, 2730–2734.

- (78) Rajkovic, S.; Kallay, C.; Serenyi, R.; Malandrinos, G.; Hadjiliadis, N.; Sanna, D.; Sovago, I. *Dalton Trans.* **2008**, 5059–5071.
- (79) Sovago, I.; Osz, K. *Dalton Trans.* **2006**, 3841–3854.
- (80) Stern, C. A.; Gennaro, A. M.; Levstein, P. R.; Calvo, R. J. *Phys. Condens. Matter* **1989**, *1*, 637–642.
- (81) Anderson, P. W. *Phys. Soc. Jpn.* **1954**, *9*, 316–339.
- (82) Glaser, T.; Heidemeier, M.; Hahn, F. E.; Pape, T.; Lugger, T. Z. *Naturforsch.* **2003**, *58b*, 505–510.
- (83) Conato, Ch.; Kamysz, W.; Kozlowski, H.; Luczkowski, M.; Maćkiewicz, Z.; Młynarz, P.; Remelli, M.; Valensin, D.; Valensin, G. *J. Chem. Soc., Dalton Trans.* **2002**, 3939–3944.
- (84) Sanna, D.; Micera, G.; Kallay, C.; Rigo, V.; Sovago, I. *Dalton Trans.* **2004**, 2702–2707.
- (85) Kallay, C.; Varnagy, K.; Malandrinos, G.; Hadjiliadis, N.; Sanna, D.; Sovago, I. *Dalton Trans.* **2006**, 4545–4552.
- (86) Boka, B.; Maryi, A.; Sovago, I.; Hadjiliadis, N. *J. Inorg. Biochem.* **2004**, *98*, 113–122.
- (87) Casolaro, M.; Chelli, M.; Ginanneschi, M.; Laschi, F.; Messori, L.; Muniz-Miranda, M.; Papini, A. M.; Kowalik-Jankowska, T.; Kozlowski, H. *J. Inorg. Biochem.* **2002**, *89*, 181–190.
- (88) Sigel, H.; Martin, R. B. *Chem. Rev.* **1982**, *82*, 385–426.
- (89) Stadtman, E. R.; Berlett, B. S. *Chem. Res. Toxicol.* **1997**, *10*, 485–494.
- (90) Levine, R. L.; Stadtman, E. R. *Exp. Gerontol.* **2001**, *36*, 1495–1502.
- (91) Beal, M. F. *Free Radical Biol. Med.* **2002**, *32*, 797–803.
- (92) Berlett, B. S.; Stadtman, E. R. *J. Biol. Chem.* **1997**, *272*, 20313–20316.
- (93) Davies, K. J. *J. Biol. Chem.* **1987**, *262*, 9895–9901.
- (94) Mirzaei, H.; Regnier, F. J. *J. Chromatogr. B.* **2008**, *873*, 8–14.
- (95) Nair, U.; Bartsch, H.; Nair, J. *Free Radical Biol. Med.* **2007**, *43*, 1109–1120.
- (96) Lovell, M. A.; Markesbery, W. R. *Nucleic Acids Res.* **2007**, *35*, 7497–7504.
- (97) Stadtman, E. R. *Annu. Rev. Biochem.* **1993**, *62*, 797–821.
- (98) Stadtman, E. R. *Free Radical Biol. Med.* **1990**, *9*, 315–325.
- (99) Hawkins, C. L.; Davies, M. J. *Biochim. Biophys. Acta* **1997**, *1360*, 84–96.
- (100) Lim, J.; Vachet, R. *Anal. Chem.* **2003**, *75*, 1164–1172.
- (101) Li, S.; Nguyen, T. H.; Schoneich, C.; Borchardt, R. T. *Biochemistry* **1995**, *34*, 5762–5772.
- (102) Zhao, F.; Ghezzi-Schoneich, E.; Aced, G. I.; Hong, J.; Milby, T.; Schoneich, C. *J. Biol. Chem.* **1997**, *272*, 9019–9029.
- (103) Bridgewater, J. D.; Vachet, R. W. *Anal. Biochem.* **2005**, *341*, 122–130.
- (104) Bridgewater, J. D.; Vachet, R. W. *Anal. Chem.* **2005**, *77*, 4649–4653.
- (105) Pan, H.; Chen, K.; Chu, L.; Kinderman, F.; Apostol, I.; Huang, G. *Protein Sci.* **2009**, *18*, 424–433.
- (106) Liu, D.; Ren, D.; Huang, H.; Dankberg, J.; Rosenfeld, R.; Cocco, M. J.; Li, L.; Brems, D. N.; Remmele, R. L., Jr. *Biochemistry* **2008**, *47*, 5088–5100.
- (107) Chumsae, C.; Gaza-Bulseco, G.; Sun, J.; Liu, H. *J. Chromatogr. B: Anal. Technol. Biomed. Life. Sci.* **2007**, *850*, 285–294.
- (108) Luo, Q.; Joubert, M. K.; Stevenson, R.; Ketchem, R. R.; Narhi, L. O.; Wypych, J. *J. Biol. Chem.* **2011**, *286*, 25134–25144.
- (109) Schoneich, Ch. *Biochim. Biophys. Acta* **2005**, *1703*, 111–119.
- (110) Xu, G.; Chance, M. R. *Chem. Rev.* **2007**, *107*, 3514–3543.
- (111) Ji, J. A.; Zhang, B.; Cheng, W.; Wang, Y. J. *J. Pharm. Sci.* **2009**, *98*, 4485–4500.
- (112) Bridgewater, J. D.; Lim, J.; Vachet, R. W. *J. Am. Soc. Mass Spectrom.* **2006**, *17*, 1552–1559.
- (113) Katiaho, T.; Eberlin, N. M.; Vainiotalo, P.; Kostaiainen, R. J. *J. Am. Soc. Mass Spectrom.* **2000**, *11*, 526–535.
- (114) Sun, H.; Gao, J.; Ferrington, D. A.; Biesiada, H.; Williams, T. D.; Squier, T. C. *Biochemistry* **1999**, *30*, 105–112.
- (115) Moskovitz, J.; Bar-Noy, S.; Williams, W. M.; Requena, J.; Berlett, B. S.; Stadtman, E. R. *Proc. Natl. Acad. Sci. U.S.A.* **2001**, *89*, 12921–12925.